

# New aspects of leptogenesis bounds

Steve Blanchet<sup>a</sup> and Pasquale Di Bari<sup>b</sup>

<sup>a</sup>*Max-Planck-Institut für Physik (Werner-Heisenberg-Institut)  
Föhringer Ring 6, 80805 München, Germany*

<sup>b</sup>*INFN, Sezione di Padova, Dipartimento di Fisica Galileo Galilei  
Via Marzolo 8, I-35131 Padua, Italy*

October 22, 2018

## Abstract

We present a general analysis that reveals new aspects of the leptogenesis bounds on neutrino masses and on the reheat temperature of the Universe. After revisiting a known effect coming from an unbounded term in the total  $CP$  asymmetry, we show that an unbounded term in the flavored  $CP$  asymmetries has a stronger impact. It relaxes the lower bound on the reheat temperature down to  $10^8$  GeV for  $(M_2 - M_1)/M_1 = \mathcal{O}(1 - 100)$  and for a mild tuning of the parameters in the see-saw orthogonal matrix. We also consider the effect of the Higgs asymmetry, showing that it lowers the upper bound on the neutrino masses in the so-called fully flavored regime where classic Boltzmann equations can be used. Imposing independence of the initial conditions contributes to lower the upper bound on neutrino masses as well. We study the conditions for the validity of the usual  $N_1$ -dominated scenario and for the applicability of the lower bound on the lightest right-handed (RH) neutrino mass  $M_1$ . We find that except for the two effective RH neutrino scenario, recovered for  $M_3 \gg 10^{14}$  GeV, and for values  $M_2 < \mathcal{O}(10^{11}$  GeV), the final asymmetry is more naturally dominated by the contribution from  $N_2$ -decays. Finally, we confirm in a general way that going beyond the hierarchical limit, the effect of washout addition makes the lower bound on  $M_1$  more stringent for  $(M_2 - M_1)/M_1 = \mathcal{O}(0.1)$ .

# 1 Introduction

Leptogenesis [1] provides an elegant solution to the problem of the non-observation of primordial antimatter in the Universe. An appealing feature of this mechanism is that it relies on a minimal extension of the Standard Model (SM) where RH neutrinos are added to the Lagrangian. In the see-saw limit [2], small neutrino masses can be naturally accommodated in agreement with the data. Considering, for definiteness, the simplest and best motivated case of three additional RH neutrinos, only few of the eighteen new parameters, three neutrino masses, three mixing angles and three  $CP$  violating phases, are or can hopefully be probed in neutrino experiments. The remaining 9 ‘high-energy’ parameters are out of reach in low energy experiments. In this respect, leptogenesis represents also an important cosmological tool to access information on this ‘dark side’ of the see-saw parameter space.

In an unflavored analysis and in a traditional  $N_1$ -dominated scenario, where it is assumed that the final asymmetry is dominantly produced from the lightest RH neutrino decays, one finds a lower bound on the lightest RH neutrino mass  $M_1$  [3, 4]. This is given by  $M_1 \gtrsim 3 \times 10^9$  GeV [5, 6] at the onset of the strong washout regime, where the final asymmetry does not depend on the initial conditions. This lower bound also implies an associated lower bound on the reheat temperature,  $T_{\text{reh}} \gtrsim 1.5 \times 10^9$  GeV [7, 8, 6]. In addition an upper bound on the neutrino masses,  $m_i \lesssim 0.1$  eV, holds as well [9].

A mild hierarchy in the spectrum of the RH neutrino masses, such that  $M_2 \gtrsim 3 M_1$ , is a necessary condition for the validity of the  $N_1$ -dominated scenario but is not sufficient. Indeed, upon closer inspection, the observed asymmetry can still be generated from the decays of the next-to-lightest RH neutrinos, realizing a  $N_2$ -dominated scenario [5]. The lower bound on  $M_1$  is replaced by a lower bound on  $M_2$  but this still implies a lower bound on  $T_{\text{reh}}$ . It is therefore more correct to say that leptogenesis yields a lower bound on  $T_{\text{reh}}$  rather than on  $M_1$ .

Even when flavor effects are considered [10, 11] (see also [12, 13]), the lower bound on  $T_{\text{reh}}$  has been found not to change [6]. On the other hand they induce other important modifications. First, the final asymmetry receives an additional contribution that also depends on neutrino mixing parameters [10, 14] and an interesting feature is that such an additional contribution can originate solely by low-energy (Dirac or Majorana) phases [10] and can even explain the whole observed asymmetry [6, 15, 16, 17, 18, 19]. Second, flavor effects can relax the stringent upper bound on the neutrino masses,  $m_i \lesssim 0.1$  eV, holding in the unflavored regime when a hierarchical heavy neutrino mass spectrum is assumed [9]. In [11], it was found that flavor effects completely erase this upper bound. However,

in [20], it was pointed out that this conclusion relies on the use of classical Boltzmann equations beyond their range of validity and has therefore to be checked within a more general description making use of density matrix equations. In [21] it was found that using classic Boltzmann equations neutrino masses as large as  $2\text{ eV}$  are possible, a value larger than the upper bound holding in the unflavored regime and than the current upper bound from cosmological observations. A similar conclusion has been recently obtained in [22] as well.

Many of these results have been obtained employing different assumptions or restrictions in the parameter space. In this paper we revisit in detail the leptogenesis bounds still assuming classical Boltzmann equations and the  $N_1$ -dominated scenario but without further restrictions on the parameter space and relaxing many assumptions that are usually made. For example, we find more general conditions for the validity of the  $N_1$ -dominated scenario. In general, our analysis reveals various new aspects including effects confirming the necessity to go beyond a classical Boltzmann kinetic approach to solve the problem of the upper bound on the neutrino masses.

In Section 2 we set up the general notation. In Section 3 we show that the final asymmetry can be written as the sum of different contributions acting independently of each other. The first step is to distinguish between a contribution from the lightest RH neutrino decays and a contribution from the heavier RH neutrino decays, just two in our case. In a traditional  $N_1$ -dominated scenario the first one is dominant. This can be still conveniently re-cast as the sum of an unflavored term plus a flavored term. Finally, the unflavored term can be further decomposed into a piece proportional to a contribution to the total  $CP$  asymmetry respecting the usual upper bound [23, 3] and into a term that is not upper bounded but vanishes when  $M_2 = M_3$ . If  $M_2 \neq M_3$ , this term is typically strongly suppressed when a mild hierarchy is assumed and barring a fine-tuned choice of the parameters [24, 25, 5]. Analogously, we recast also the flavored  $CP$  asymmetries as the sum of an upper-bounded term plus an unbounded extra-term that has been neglected in previous works but that proves to be important in interesting cases.

In the end of Section 3 we review, as a starting point for our analysis, the neutrino mass bounds that arise in the minimal scenario, that we call ‘vanilla leptogenesis’, when all simplifications are made at once: the heavier RH neutrino contribution, the flavored terms and the extra-term to the total  $CP$  asymmetry are neglected and the hierarchical limit is taken. In this case the final asymmetry depends only on 6 parameters [7, 5].

In Section 4 we show the role played by the unbounded term in the total  $CP$  asymmetry of the lightest RH neutrino,  $\varepsilon_1$ , that has to be considered when  $M_2 \neq M_3$  [24, 25, 5]. We study its effect on the bounds in a quite conservative mild hierarchical limit  $M_2 \simeq$

$3M_1$ , showing how a rotation in the complex 2-3 plane is the most effective ingredient in enhancing this term and showing that the bounds get modified only for fine tuned parameter choices. Our analysis shows moreover that this extra-term acts independently of flavor effects.

In Section 5 we study how the bounds change when flavor effects are taken into account and, interestingly, we show that a so far neglected term in the flavored  $CP$  asymmetries is actually able to relax the lower bound on the reheating temperature in presence of wash-out. In the case of the upper bound on the absolute neutrino mass scale, we show that this is sensitive to a variation of different assumptions and conditions. We also show that, taking into account the Higgs asymmetry then, within the validity of classical Boltzmann equations, one cannot say whether the bound  $m_1 \lesssim 0.1 \text{ eV}$  holding in the unflavored regime is evaded. This conclusion is strengthened when independence of the initial conditions is imposed.

In Section 6 we consider the contribution from the two heavier RH neutrinos, including flavor effects and still assuming the hierarchical limit, showing a (non-trivial) sufficient condition for the  $N_1$ -dominated scenario to hold.

Finally, in Section 7, we show how the neutrino mass bounds change going beyond the limit of hierarchical RH neutrinos when flavor effects are included. Contrarily to a naive expectation, we show that the allowed region, instead of getting enlarged, actually shrinks when mild degeneracies for the heavy neutrinos masses are considered. The bounds get relaxed only when the heavy neutrino mass degeneracies are much smaller than those of the light neutrinos.

## 2 General set-up

Leptogenesis is based on a popular extension of the Standard Model,

$$\mathcal{L} = \mathcal{L}_{\text{SM}} + i\overline{N_{Ri}}\gamma_\mu\partial^\mu N_{Ri} - h_{\alpha i}\overline{\ell_{L\alpha}}N_{Ri}\tilde{\Phi} - \frac{1}{2}M_i\overline{N_{Ri}^c}N_{Ri} + h.c. \quad (i = 1, 2, 3, \quad \alpha = e, \mu, \tau), \quad (1)$$

where three RH neutrinos  $N_{Ri}$ , with a Majorana mass term  $M$  and Yukawa couplings  $h$ , are added. After spontaneous symmetry breaking, a Dirac mass term  $m_D = v h$ , is generated by the vev  $v = 174 \text{ GeV}$  of the Higgs boson. In the see-saw limit,  $M \gg m_D$ , the spectrum of neutrino mass eigenstates splits in two sets: 3 very heavy neutrinos,  $N_1, N_2$  and  $N_3$  respectively with masses  $M_1 \leq M_2 \leq M_3$  almost coinciding with the eigenvalues of  $M$ , and 3 light neutrinos with masses  $m_1 \leq m_2 \leq m_3$ , the eigenvalues of the light

neutrino mass matrix given by the see-saw formula [2],

$$m_\nu = -m_D \frac{1}{M} m_D^T. \quad (2)$$

Neutrino oscillation experiments measure two neutrino mass-squared differences. For normal schemes one has  $m_3^2 - m_2^2 = \Delta m_{\text{atm}}^2$  and  $m_2^2 - m_1^2 = \Delta m_{\text{sol}}^2$ , whereas for inverted schemes one has  $m_3^2 - m_2^2 = \Delta m_{\text{sol}}^2$  and  $m_2^2 - m_1^2 = \Delta m_{\text{atm}}^2$ . For  $m_1 \gg m_{\text{atm}} \equiv \sqrt{\Delta m_{\text{atm}}^2 + \Delta m_{\text{sol}}^2} = (0.050 \pm 0.001) \text{ eV}$  [26] the spectrum is quasi-degenerate, while for  $m_1 \ll m_{\text{sol}} \equiv \sqrt{\Delta m_{\text{sol}}^2} = (0.0088 \pm 0.0001) \text{ eV}$  [26] it is fully hierarchical (normal or inverted). The most stringent upper bound on the absolute neutrino mass scale comes from cosmological observations. Recently, quite a conservative upper bound,

$$m_1 < 0.2 \text{ eV} \quad (95\% \text{ CL}), \quad (3)$$

has been obtained by the WMAP collaboration combining CMB, baryon acoustic oscillations and supernovae type Ia observations [27].

With leptogenesis, this simple extension of the Standard Model is also able to explain the observed baryon asymmetry of the Universe [27]

$$\eta_B^{\text{CMB}} = (6.2 \pm 0.15) \times 10^{-10}. \quad (4)$$

It is widely known that, in order to generate a baryon asymmetry in the early Universe, one needs to satisfy the three Sakharov conditions [28]. At temperatures  $T \gtrsim 100 \text{ GeV}$ , baryon number is violated by the non-perturbative sphaleron processes [29]. Moreover  $CP$  is violated in the decays of the heavy RH neutrinos. Indeed the Dirac mass matrix is in general complex and this provides a natural source of  $CP$  violation. At the same time departure from thermal equilibrium occurs in the decays of the heavy RH neutrinos as well. This can be conveniently quantified in terms of the decay parameters, defined as  $K_i \equiv \tilde{\Gamma}_i / H_{T=M_i}$ , given by the ratio of the decay widths to the expansion rate when the RH neutrinos become non-relativistic. The decay parameters can be expressed in terms of the Yukawa couplings by

$$K_i = \frac{\tilde{m}_i}{m_\star}, \quad \text{where} \quad \tilde{m}_i \equiv \frac{(m_D^\dagger m_D)_{ii}}{M_i} \quad (5)$$

are the effective neutrino masses and  $m_\star$  is the equilibrium neutrino mass [7] given by

$$m_\star \equiv \frac{16 \pi^{5/2} \sqrt{g_*}}{3 \sqrt{5}} \frac{v^2}{M_{\text{Pl}}} \simeq 1.08 \times 10^{-3} \text{ eV}. \quad (6)$$

There are two ways how  $CP$  violation can manifest itself. A first one is given by having a decay rate of  $N_i$  into leptons,  $\Gamma_i$ , different from the decay rate into anti-leptons,  $\bar{\Gamma}_i$ . This is parameterized by the total  $CP$  asymmetries

$$\varepsilon_i \equiv -\frac{\Gamma_i - \bar{\Gamma}_i}{\Gamma_i + \bar{\Gamma}_i}. \quad (7)$$

A perturbative calculation from the interference of tree level with one loop self-energy and vertex diagrams gives [30]

$$\varepsilon_i = \frac{3}{16\pi} \sum_{j \neq i} \frac{\text{Im} [(h^\dagger h)_{ij}^2]}{(h^\dagger h)_{ii}} \frac{\xi(x_j/x_i)}{\sqrt{x_j/x_i}}, \quad (8)$$

having introduced [9]

$$\xi(x) = \frac{2}{3} x \left[ (1+x) \ln \left( \frac{1+x}{x} \right) - \frac{2-x}{1-x} \right]. \quad (9)$$

A second way [10] is given by the possibility that in general, indicating with  $|\ell_i\rangle$  the final lepton quantum state and with  $|\bar{\ell}'_i\rangle$  the final anti-lepton quantum state, one has  $|\ell_i\rangle \neq CP|\bar{\ell}'_i\rangle$ . This can be easily understood when the flavor composition of the final lepton state is considered. Indeed, introducing the projectors on the flavor eigenstates, they can be written like the sum of two terms,

$$P_{i\alpha} \equiv |\langle \ell_i | \ell_\alpha \rangle|^2 = P_{i\alpha}^0 + \frac{\Delta P_{i\alpha}}{2} \quad (10)$$

$$\bar{P}_{i\alpha} \equiv |\langle \bar{\ell}'_i | \bar{\ell}_\alpha \rangle|^2 = P_{i\alpha}^0 - \frac{\Delta P_{i\alpha}}{2}. \quad (11)$$

The first term is the tree level contribution and is common to both projectors but the second term, from loop corrections, changes sign and gives rise to a different flavor composition when  $\Delta P_{i\alpha} \neq 0$ . These two  $CP$  violating effects translate respectively in two separate terms in the flavored  $CP$  asymmetries,

$$\varepsilon_{i\alpha} \equiv -\frac{\Gamma_{i\alpha} - \bar{\Gamma}_{i\alpha}}{\Gamma_i + \bar{\Gamma}_i} = P_{i\alpha}^0 \varepsilon_{i\alpha} + \frac{\Delta P_{i\alpha}}{2}, \quad (12)$$

where  $\Gamma_{i\alpha} \equiv P_{i\alpha} \Gamma_i$  and  $\bar{\Gamma}_{i\alpha} \equiv \bar{P}_{i\alpha} \bar{\Gamma}_i$ . The flavored  $CP$  asymmetries can be calculated using [30]

$$\varepsilon_{i\alpha} = \frac{3}{16\pi(h^\dagger h)_{ii}} \sum_{j \neq i} \left\{ \text{Im} [h_{\alpha i}^* h_{\alpha j} (h^\dagger h)_{ij}] \frac{\xi(x_j/x_i)}{\sqrt{x_j/x_i}} + \frac{2}{3(x_j/x_i - 1)} \text{Im} [h_{\alpha i}^* h_{\alpha j} (h^\dagger h)_{ji}] \right\}. \quad (13)$$

The second  $CP$  violating contribution yields an additional contribution to the final asymmetry only if the flavor composition plays a role in the determination of the final asymmetry. This depends on the effectiveness of the charged lepton interactions implied by the term  $f_\alpha \bar{\ell}_{L\alpha} e_{R\alpha} \Phi$  in the Lagrangian, which is diagonal in flavor space. The latter implies that the processes  $\ell_\alpha \bar{e}_\alpha \leftrightarrow \Phi$  and  $\ell_\alpha \bar{e}_\alpha \leftrightarrow \Phi A^a$  and the  $CP$  conjugated, (where  $A^a$  ( $a = 1, 2, 3$ ) are the  $SU(2)_L$  gauge bosons) occur at a rate  $\Gamma_\alpha \simeq 5 \times 10^{-3} T f_\alpha^2$  ( $\alpha = e, \mu, \tau$ ) [31]. If these processes are effective, then they measure the flavor composition of the final leptons and this becomes a relevant ingredient in the determination of the final asymmetry if a second condition is fulfilled as well, as we will comment.

In the hierarchical limit the decays of just one species of RH neutrino, the lightest [1] or the next-to-lightest [5], dominantly contribute to the final asymmetry. If  $\Gamma_\alpha \ll \Gamma_{\text{ID}}^i$  ( $i = 1, 2$ ) during the relevant period of the asymmetry generation, where  $\Gamma_{\text{ID}}^i$  denotes the inverse-decay rate, then the coherence of the lepton states is preserved on average between a decay and a subsequent inverse decays and the unflavored regime, where flavor effects are negligible, holds. This requirement implies [20]

$$M_i \gtrsim 5 \times 10^{11} \text{ GeV}. \quad (14)$$

In this case an approximate set of Boltzmann equations is given by

$$\frac{dN_{N_i}}{dz} = -D_i (N_{N_i} - N_{N_i}^{\text{eq}}), \quad i = 1, 2, 3 \quad (15)$$

$$\frac{dN_{B-L}}{dz} = \sum_{i=1}^3 \varepsilon_i D_i (N_{N_i} - N_{N_i}^{\text{eq}}) - N_{B-L} [\Delta W(z) + \sum_i W_i^{\text{ID}}(z)], \quad (16)$$

where  $z \equiv M_1/T$  and where we indicated with  $N_X$  any particle number or asymmetry  $X$  calculated in a portion of co-moving volume containing one heavy neutrino in ultra-relativistic thermal equilibrium, so that  $N_{N_i}^{\text{eq}}(T \gg M_i) = 1$ . With this convention, the predicted baryon-to-photon ratio  $\eta_B$  is related to the final value of the final  $B - L$  asymmetry by the relation

$$\eta_B = a_{\text{sph}} \frac{N_{B-L}^{\text{f}}}{N_\gamma^{\text{rec}}} \simeq 0.96 \times 10^{-2} N_{B-L}^{\text{f}}, \quad (17)$$

where  $N_\gamma^{\text{rec}} \simeq 37$ , and  $a_{\text{sph}} = 28/79$ . Defining  $x_i \equiv M_i^2/M_1^2$  and  $z_i \equiv z \sqrt{x_i}$ , the decay factors are given by

$$D_i \equiv \frac{\Gamma_{\text{D},i}}{H z} = K_i x_i z \left\langle \frac{1}{\gamma_i} \right\rangle, \quad (18)$$

where  $H$  is the expansion rate. The total decay rates,  $\Gamma_{\text{D},i} \equiv \Gamma_i + \bar{\Gamma}_i$ , are the product of the decay widths times the thermally averaged dilation factors  $\langle 1/\gamma \rangle$ , given by the ratio

$\mathcal{K}_1(z)/\mathcal{K}_2(z)$  of the modified Bessel functions. The equilibrium abundance and its rate are also expressed through the modified Bessel functions,

$$N_{N_i}^{\text{eq}}(z_i) = \frac{1}{2} z_i^2 \mathcal{K}_2(z_i) \quad , \quad \frac{dN_{N_i}^{\text{eq}}}{dz_i} = -\frac{1}{2} z_i^2 \mathcal{K}_1(z_i) . \quad (19)$$

After proper subtraction of the resonant contribution from  $\Delta L = 2$  processes [32], the inverse decay washout terms are simply given by

$$W_i^{\text{ID}}(z) = \frac{1}{4} K_i \sqrt{x_i} \mathcal{K}_1(z_i) z_i^3 . \quad (20)$$

The washout term  $\Delta W(z)$  is the non-resonant  $\Delta L = 2$  processes contribution. It gives a non-negligible effect only at  $z \gg 1$  and in this case it can be approximated as [7]

$$\Delta W(z) \simeq \frac{\omega}{z^2} \left( \frac{M_1}{10^{10} \text{ GeV}} \right) \left( \frac{\bar{m}^2}{\text{eV}^2} \right) , \quad (21)$$

where  $\omega \simeq 0.186$  and  $\bar{m}^2 \equiv m_1^2 + m_2^2 + m_3^2$ . Notice that we are neglecting  $\Delta L = 1$  scatterings [33, 14], giving a correction to a level less than  $\sim 10\%$  [6], thermal corrections [8], giving relevant (though with big theoretical uncertainties) corrections only in the weak washout, and spectator processes [34, 35], that produce corrections to a level less than  $\sim 20\%$  [35].

On the other hand, if the charged lepton Yukawa interactions are in equilibrium ( $\Gamma_\alpha > H$ ) and faster than inverse decays, i.e.

$$\Gamma_\alpha \gtrsim \Gamma_{\text{ID}}^i , \quad (22)$$

during the relevant period of the asymmetry generation, then lepton quantum states lose coherence between the production at decay and the subsequent absorption in inverse processes. If the quantum state becomes completely incoherent and is fully projected on one of the flavor eigenstates, each lepton flavor eigenstate  $\ell_\alpha$  can be treated as a statistically independent particle species and a ‘fully flavored regime’ is obtained. Note that one has to distinguish a two-flavor regime, for  $M_i \gtrsim 10^9 \text{ GeV}$ , such that the condition Eq. (22) is satisfied only for  $\alpha = \tau$ , and a three-flavor regime, where it applies also to  $\alpha = \mu$ .

In the fully flavored regime (two or three flavors), classical Boltzmann equations can be still used like in the unflavored regime, with the difference, in general, that now each single flavor asymmetry has to be tracked independently. Since sphaleron processes conserve the quantities  $\Delta_\alpha \equiv B/3 - L_\alpha$  ( $\alpha = e, \mu, \tau$ ), these are the convenient independent variables



to be used in the set of Boltzmann equations that can be written as

$$\frac{dN_{N_i}}{dz} = -D_i (N_{N_i} - N_{N_i}^{\text{eq}}) \quad (i = 1, 2, 3) \quad (23)$$

$$\frac{dN_{\Delta_\alpha}}{dz} = \sum_i \varepsilon_{i\alpha} D_i (N_{N_i} - N_{N_i}^{\text{eq}}) - \sum_{i,\beta} P_{i\alpha}^0 (C_{\alpha\beta}^\ell + C_\beta^H) W_i^{\text{ID}} N_{\Delta_\beta}, \quad (24)$$

where we are using the same approximations as in the unflavored case but neglecting the non-resonant  $\Delta L = 2$  term, since this counts only for  $M_1 \gtrsim 10^{14}$  GeV ( $m_{\text{atm}}^2 / \sum_i m_i^2$ ) like also a contribution from  $\Delta L = 0$  processes that one has to consider in the flavored case. Notice that the final  $B - L$  asymmetry is now calculated as  $N_{B-L}^f = \sum_\alpha N_{\Delta_\alpha}^f$ .

The  $C^\ell$  matrix [12] relates the asymmetries stored in lepton doublets,  $\ell_\alpha$ , to the asymmetries  $\Delta_\alpha \equiv B/3 - L_\alpha$  asymmetries and is given, in a two-flavor regime, by [14]

$$C^\ell = \frac{1}{316} \begin{pmatrix} 270 & -32 \\ -17 & 208 \end{pmatrix}. \quad (25)$$

The  $C^H$  matrix takes into account the washout due to the asymmetry stored in the Higgs field [10] and is given by

$$C^H = \frac{1}{158} (41, 56). \quad (26)$$

The Higgs asymmetry has been neglected so far but, as we will see, it has a relevant effect on the upper bound on the neutrino masses. Indeed the sum of the two matrices gives

$$C \equiv C^\ell + C^H \simeq \begin{pmatrix} 1.11 & 0.25 \\ 0.21 & 1.01 \end{pmatrix}. \quad (27)$$

The off-diagonal terms give a small effect in the calculation of the final asymmetry [14] and therefore, in the end, one can safely use the approximation  $C \simeq I$  in the derivation of the bounds. In Section 5 we will compare the results when the Higgs asymmetry is neglected, when it is taken into account and when one uses the approximation  $C \simeq I$ , showing that the latter works very well justifying its use for the remainder of the paper.

Taking for simplicity the two flavor case, it is instructive to sum over the flavor Eq. (24), obtaining

$$\frac{dN_{B-L}}{dz} \simeq \sum_{i=1}^3 \varepsilon_i D (N_{N_i} - N_{N_i}^{\text{eq}}) - \frac{1}{2} N_{B-L} \sum_{i=1}^3 W_i^{\text{ID}} + \frac{1}{2} [N_{\Delta_\alpha} - N_{\Delta_\beta}] \sum_{i=1}^3 (P_{i\alpha}^0 - P_{i\beta}^0) W_i^{\text{ID}}. \quad (28)$$

This equation clearly shows that when the washout vanishes there must be no difference between the unflavored and the fully flavored regime. Therefore, the lower bounds on

$M_1$  and on  $T_{\text{reh}}$  obtained in the limit of no-washout, rigorously for an initial thermal abundance and approximately for an initial vanishing abundance, do not change when flavor effects are taken into account [6].

A convenient parametrization of the Dirac mass matrix is obtained in terms of the orthogonal matrix [36]

$$m_D = U D_m^{1/2} \Omega D_M^{1/2}, \quad (29)$$

where we defined  $D_m \equiv \text{diag}(m_1, m_2, m_3)$  and  $D_M \equiv \text{diag}(M_1, M_2, M_3)$ . The matrix  $U$  diagonalizes the light neutrino mass matrix  $m_\nu$ , such that  $U^\dagger m_\nu U^* = -D_m$ , and it can be identified with the lepton mixing matrix in a basis where the charged lepton mass matrix is diagonal. We will adopt the parametrization [37]

$$U = \begin{pmatrix} c_{12} c_{13} & s_{12} c_{13} & s_{13} e^{-i\delta} \\ -s_{12} c_{23} - c_{12} s_{23} s_{13} e^{i\delta} & c_{12} c_{23} - s_{12} s_{23} s_{13} e^{i\delta} & s_{23} c_{13} \\ s_{12} s_{23} - c_{12} c_{23} s_{13} e^{i\delta} & -c_{12} s_{23} - s_{12} c_{23} s_{13} e^{i\delta} & c_{23} c_{13} \end{pmatrix} \times \text{diag}(e^{i\frac{\phi_1}{2}}, e^{i\frac{\phi_2}{2}}, 1), \quad (30)$$

where  $s_{ij} \equiv \sin \theta_{ij}$ ,  $c_{ij} \equiv \cos \theta_{ij}$  and, neglecting the statistical errors, we will use  $\theta_{12} = \pi/5$  and  $\theta_{23} = \pi/4$ , compatible with the results from neutrino oscillation experiments. Moreover, we will adopt the  $3\sigma$  range  $s_{13} = 0 - 0.20$ , allowed from a global  $3\nu$  analysis for unitary  $U$  [26], an approximation that holds with great precision in the see-saw limit with  $M_i \gg 100 \text{ GeV}$ . With the adopted convention for the light neutrino masses,  $m_1 < m_2 < m_3$ , this parametrization is valid only for normal hierarchy, while for inverted hierarchy one has to perform a column cyclic permutation. In a general analysis, leptogenesis bounds are not depending on the scheme, normal or inverted, but in restricted scenarios, like in the effective two RH neutrino scenario where the third is very heavy and decouples or in ‘Dirac phase leptogenesis’ [19], differences can arise and depend on flavor effects. We will signal these differences in our analysis.

It will also prove useful to introduce the following parametrization for the see-saw orthogonal matrix in terms of complex rotations

$$\Omega(\omega_{21}, \omega_{31}, \omega_{32}) = \text{diag}(\pm, \pm, \pm) R_{12}(\omega_{21}) R_{13}(\omega_{31}) R_{23}(\omega_{32}), \quad (31)$$

where

$$R_{12} = \begin{pmatrix} \pm\sqrt{1-\omega_{21}^2} & -\omega_{21} & 0 \\ \omega_{21} & \pm\sqrt{1-\omega_{21}^2} & 0 \\ 0 & 0 & 1 \end{pmatrix}, \quad R_{13} = \begin{pmatrix} \pm\sqrt{1-\omega_{31}^2} & 0 & -\omega_{31} \\ 0 & 1 & 0 \\ \omega_{31} & 0 & \pm\sqrt{1-\omega_{31}^2} \end{pmatrix}, \quad R_{23} = \begin{pmatrix} 1 & 0 & 0 \\ 0 & \pm\sqrt{1-\omega_{32}^2} & -\omega_{32} \\ 0 & \omega_{32} & \pm\sqrt{1-\omega_{32}^2} \end{pmatrix} \quad (32)$$

and where the overall sign takes into account the possibility of a parity transformation as well. Notice that, using the orthogonal parametrization, Eq. (29), the effective neutrino

masses, and consequently the decay parameters, can be expressed as linear combinations of the neutrino masses [38, 7], such that  $\tilde{m}_i = \sum_j m_j |\Omega_{ji}^2|$ . Notice that the orthogonality of  $\Omega$  is equivalent to the see-saw relation for the light neutrino masses and in particular one has that  $\text{Re}[\Omega_{ij}^2]$  is the contribution to  $m_i$  from the term  $\propto 1/M_j$ . Therefore, large absolute values of the  $\Omega$  entries imply a strong fine tuning not only because they require phase cancelations but also because they imply that neutrino masses are much lighter than terms  $\propto m_D^2/M$  because of sign cancelations. Therefore, such choices tend to transfer the explanation of neutrino lightness from the see-saw mechanism to some other mechanism that has to explain the fine-tuned cancelations. The interest for considering models with very large  $|\Omega_{ij}|$  is merely phenomenological since they make possible to satisfy neutrino masses with the see-saw mechanism and at the same time to have TeV RH neutrinos with large Yukawa's, making possible to detect them in colliders [39]. This will not be our point of view in this paper and we will conventionally consider orthogonal matrices to be ‘reasonable’ if  $|\omega_{ij}| \leq 1$ , implying  $|\Omega_{ij}| \lesssim 1$ , and ‘acceptable’ if  $|\omega_{ij}| \leq 10$ , implying  $|\Omega_{ij}| \lesssim 10$ . These will be the two benchmark cases that we will adopt in the plots.

To conclude this Section we just want to recall the particularly relevant case of two effective RH neutrinos, obtained in the limit where  $M_3 \gg 10^{14}$  GeV [40, 41, 42]. In this limit the orthogonal matrix necessarily collapses into

$$\Omega = \begin{pmatrix} 0 & 0 & 1 \\ \pm\sqrt{1 - \Omega_{31}^2} & -\Omega_{31} & 0 \\ \Omega_{31} & \pm\sqrt{1 - \Omega_{31}^2} & 0 \end{pmatrix}, \quad (33)$$

corresponding to have  $\omega_{32} = 1$  and  $\omega_{21} = 1$  in the Eq. (32).

### 3 Vanilla leptogenesis

Using the approximation  $C \simeq I$ , a general solution for the final asymmetry can be written as [6]

$$N_{B-L}^f = \sum_{\alpha} N_{\Delta\alpha}^{\text{in}} e^{-[\Delta W(z) + \sum_i P_{i\alpha}^0 \int_{z_{\text{in}}}^z dz' W_i^{\text{ID}}(z')]} + \sum_{i,\alpha} \varepsilon_{i\alpha} \kappa_{i\alpha}^f, \quad (34)$$

with the final values of the 9 efficiency factors given by

$$\kappa_{i\alpha}^f(K_i, P_{i\alpha}^0) = - \int_{z_{\text{in}}}^{\infty} dz' \frac{dN_{N_i}}{dz'} e^{-[\Delta W(z) + \sum_i P_{i\alpha}^0 \int_{z'}^{\infty} dz'' W_i^{\text{ID}}(z''; K_i)]}. \quad (35)$$

This solution holds both in the fully flavored regime and in the unflavored regime, adopting the convention that when the condition (14) applies, all projectors  $P_{i\alpha}^0 = 1$ . It is indeed

easy to verify that in this case, summing over the flavor, the set of equations (24) reduces to Eq. (16). On the other hand it should be also noticed that Eq. (24) holds only if the condition (22) is respected and this, when applied to the  $N_1$  decays and inverse decays, translates into

$$M_1 \lesssim \frac{10^{12} \text{ GeV}}{2 W_1^{\text{ID}}(z_B(K_{1\alpha}))}. \quad (36)$$

For  $W_1^{\text{ID}}(z_B) \gtrsim 1$  there is an intermediate regime where the unflavored regime does not hold but at the same time the validity of the Eq. (24), and therefore of the expression (34), is not guaranteed. We will signal in the plots the results obtained in the fully flavored regime but for which the condition (36) is not satisfied. These results should be therefore checked within a more general kinetic description employing density matrix equations able to describe the regime where coherence (or decoherence) of the final lepton quantum state is only partial.

Notice that the  $N_{\Delta\alpha}^{\text{in}}$ 's are the values of possible pre-existing flavored asymmetries. In the unflavored regime  $K_1$  is the only parameter that determines whether the final asymmetry depends or not on a possible pre-existing asymmetry [9]. Taking into account flavor effects the problem is more involved and there are different issues to be considered. Here we will not face this problem and we will simply assume that the first term is negligible.

It is instructive to re-cast the Eq. (34) in an approximate way that enlightens different effects and contributions. For definiteness, we consider the two-flavor regime holding for  $M_1 \gtrsim 10^9 \text{ GeV}$ . The total  $CP$  asymmetry  $\varepsilon_1$  can be recast as [5]

$$\varepsilon_1 = \xi(x_2) \bar{\varepsilon}_1(M_1, m_1, \omega_{21}, \omega_{31}) + [\xi(x_3) - \xi(x_2)] \Delta\varepsilon_1(M_1, m_1, \Omega), \quad (37)$$

where, defining

$$\bar{\varepsilon}(M_1) \equiv \frac{3}{16\pi} \frac{M_1 m_{\text{atm}}}{v^2} \quad \text{and} \quad \beta(m_1, \omega_{21}, \omega_{31}) \equiv \frac{\sum_j m_j^2 \text{Im}(\Omega_{j1}^2)}{m_{\text{atm}} \sum_j m_j |\Omega_{j1}^2|}, \quad (38)$$

one has

$$\bar{\varepsilon}_1(M_1, m_1, \omega_{21}, \omega_{31}) = \bar{\varepsilon}(M_1) \beta(m_1, \omega_{21}, \omega_{31}) \quad (39)$$

and

$$\Delta\varepsilon_1(M_1, m_1, \Omega) = \bar{\varepsilon}(M_1) \frac{\text{Im}[\sum_h m_h \Omega_{h1}^* \Omega_{h3}]^2}{m_{\text{atm}} \tilde{m}_1}. \quad (40)$$

With these definitions, the final asymmetry can be written approximately as

$$N_{B-L}^f \simeq N_{\text{fl}} \{ \xi(x_2) \bar{\varepsilon}_1(M_1, m_1, \omega_{21}, \omega_{31}) + [\xi(x_3) - \xi(x_2)] \Delta\varepsilon_1(M_1, m_1, \Omega) \} \kappa_1^f \quad (41)$$

$$+ \frac{\Delta P_{1\alpha}(M_1, m_1, \Omega, U)}{2} [\kappa_{1\alpha}^f - \kappa_{1\beta}^f] + \sum_{\alpha} [\varepsilon_{2\alpha} \kappa_{2\alpha}^f + \varepsilon_{3\alpha} \kappa_{3\alpha}^f],$$

where  $N_{\text{fl}}$  is an effective number of flavors. In the unflavored regime one has  $N_{\text{fl}} = 1$ , and in the fully flavored regime, if both flavors experience a strong washout ( $P_{1\alpha,\beta}^0 K_1 \gg 1$ ), one has approximately  $N_{\text{fl}} \simeq 2$ , while in general  $1 \leq N_{\text{fl}} \lesssim 2$ .

The simplest scenario, that we call *vanilla leptogenesis* borrowing the name from observational cosmology, corresponds to taking all possible simplifying assumptions:

1. hierarchical limit,  $M_2 \gtrsim 3 M_1$ , so that  $\xi(x_2) \simeq 1$ ;
2. negligible contribution from the heavier RH neutrinos;
3. negligible flavor effects ( $N_{\text{fl}} = 1$  and  $\Delta P_{1\alpha} = 0$ );
4.  $M_2 = M_3$ , so that  $\xi(x_2) - \xi(x_3) = 0$ .

The calculation of the final asymmetry then simply reduces to

$$N_{B-L}^{\text{f}} \simeq \bar{\varepsilon}_1(m_1, M_1, \omega_{21}, \omega_{31}) \kappa_1^{\text{f}}(m_1, M_1, \omega_{21}, \omega_{31}), \quad (42)$$

depending only on 6 unknown parameters. The efficiency factor is well approximated by [7]

$$\kappa_1^{\text{f}}(M_1, m_1, K_1) = \kappa_1^{\text{f}}(K_1) \exp \left\{ -\frac{\omega}{z_{\text{B}}} \left( \frac{M_1}{10^{10} \text{ GeV}} \right) \left( \frac{\bar{m}}{\text{eV}} \right)^2 \right\}. \quad (43)$$

For the case of a thermal initial  $N_1$ -abundance ( $N_{N_1}^{\text{in}} = 1$ ), one has

$$\kappa_1^{\text{f}}(K_1) \simeq \kappa(K_1) \equiv \frac{2}{K_1 z_{\text{B}}(K_1)} \left[ 1 - \exp \left( -\frac{1}{2} K_1 z_{\text{B}}(K_1) \right) \right], \quad (44)$$

where  $z_{\text{B}}$  is approximately given by the expression [43]

$$z_{\text{B}}(K_1) \simeq 2 + 4 K_1^{0.13} \exp \left( -\frac{2.5}{K_1} \right). \quad (45)$$

In the relevant range  $5 \lesssim K_1 \lesssim 100$  this expression is further well approximated by the simple power-law  $\kappa_1^{\text{f}}(K_1) \simeq 0.5/K_1^{1.2}$  [44].

In the case of a vanishing initial  $N_1$ -abundance ( $N_{N_1}^{\text{in}} = 0$ ), one has to take into account both a negative and a positive contribution, such that

$$\kappa_1^{\text{f}}(K_1) = \kappa_-^{\text{f}}(K_1) + \kappa_+^{\text{f}}(K_1). \quad (46)$$

The analytic expressions for  $\kappa_-^{\text{f}}(K_1)$  and  $\kappa_+^{\text{f}}(K_1)$  can be found in [7]. Imposing that the predicted final asymmetry, Eq. (17), explains the observed one, Eq. (4), yields the condition

$$M_1 = \frac{\bar{M}}{\kappa_1^{\text{f}}(M_1, m_1, K_1) \beta(m_1, \omega_{21}, \omega_{31})}, \quad (47)$$

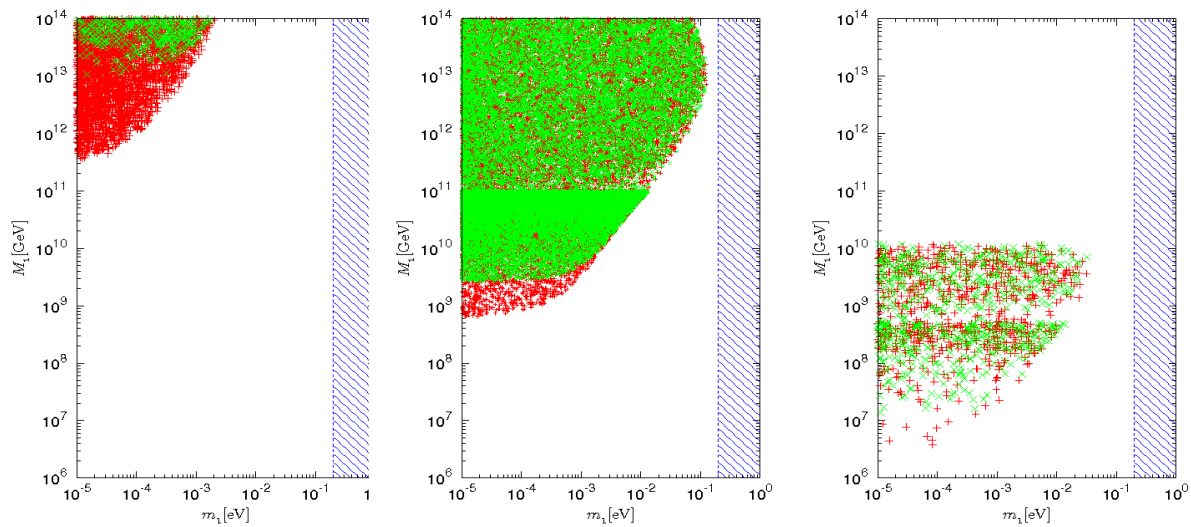


Figure 1: Vanilla leptogenesis and leptogenesis conspiracy. The allowed region in the plane  $(m_1, M_1)$  is shown for different values of  $m_{\text{atm}}$  setting the value of  $\overline{M}$  (cf. Eq. (48)). In the central panel the true measured value is considered,  $m_{\text{atm}} \simeq 0.050$  eV, while in the left and right panels two ‘wrong’ values are considered,  $m_{\text{atm}} = 10^{-4}$  eV (left) and  $m_{\text{atm}} = 10$  eV (right). In all three panels, the red crosses correspond to a thermal initial  $N_1$ -abundance while the green ones to a vanishing initial  $N_1$ -abundance. The hatched area indicates values of  $m_1$  excluded by the upper bound Eq. (3).

where we defined

$$\overline{M} \equiv \frac{16\pi}{3} \frac{N_\gamma^{\text{rec}} v^2}{a_{\text{sph}}} \frac{\eta_B^{\text{CMB}}}{m_{\text{atm}}} = (6.6 \pm 0.3) \times 10^8 \text{ GeV} \gtrsim 5.7 \times 10^8 \text{ GeV}. \quad (48)$$

The last inequality gives the  $3\sigma$  value of  $\overline{M}$  that we used in the plots to obtain the allowed region in the  $(m_1, M_1)$  plane scanning over all values of  $\omega_{21}$  and  $\omega_{31}$ . The result is shown in the central panel of Fig. 1. One can notice the presence of the usual lower bound on the lightest RH neutrino mass,  $M_1 \gtrsim 2.3 \times 10^9$  GeV for initial vanishing abundance and  $M_1 \gtrsim 5.7 \times 10^8$  GeV for initial thermal abundance [4]. This can be easily inferred from the Eq. (47) neglecting the exponential factor in Eq. (43) and using the well-known upper bound

$$\beta(m_1, \omega_{21}, \omega_{31}) \leq \frac{m_{\text{atm}}}{m_1 + m_3} f(m_1, \tilde{m}_1), \quad (49)$$

where the function  $0 \leq f(m_1, \tilde{m}_1) \leq 1$  is unity in the limit  $\tilde{m}_1/m_1 \rightarrow \infty$ , and vanishes for  $\tilde{m}_1 = m_1$ . This function can be derived analytically together with simple analytic expressions valid in particular regimes [5]. For  $m_1 \ll \tilde{m}_1 \ll m_\star$  and for initial thermal

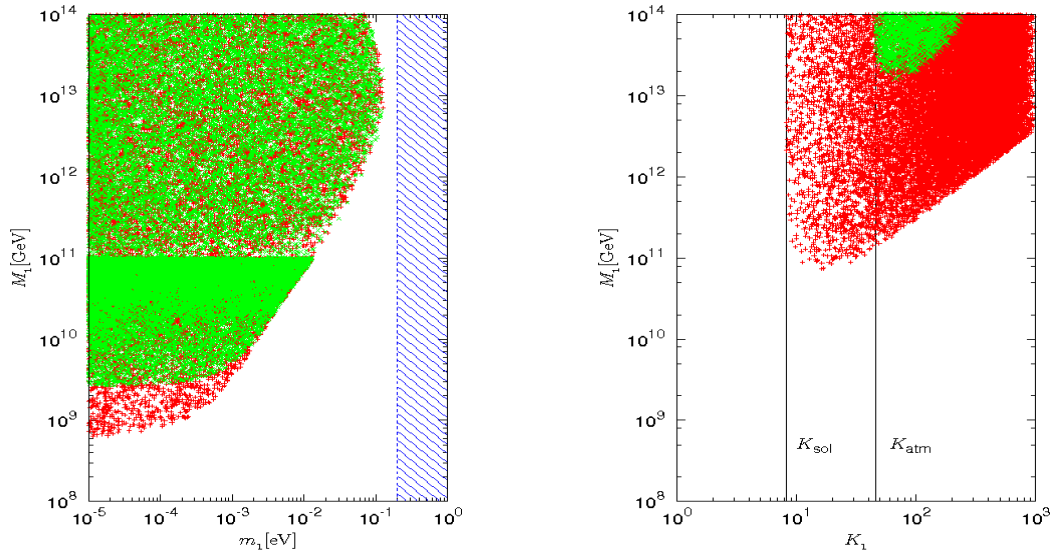


Figure 2: Allowed region in the plane  $(m_1, M_1)$  for  $\Omega = R_{13}$  (left panel), and  $M_1$  lower bound versus  $K_1$  for the effective 2 RH neutrino case obtained for  $M_3 \rightarrow \infty$  and implying  $m_1 = 0$  (right panel). In the left panel, the color coding is the same as in the previous figure. In the right panel, the red crosses correspond to normal hierarchy whereas the green ones to inverted scheme.

abundance one simply finds  $M_1 \geq \overline{M} \gtrsim 5.7 \times 10^8 \text{ GeV}$ , in agreement with the numerical result. From the central panel of Fig. 1 one can also notice that vanilla leptogenesis predicts  $m_1 \lesssim 0.12 \text{ eV}$  [9], in agreement with the current observational upper bound (cf. Eq. (3)). In the plots the hatched region indicates the excluded values. This upper bound can be derived analytically as well [7].

We performed a simple exercise showing how the allowed region in the  $(m_1, M_1)$  plane would have been for values of  $m_{\text{atm}}$  and  $m_{\text{sol}}$  different from the true measured ones. We kept the ratio  $m_{\text{atm}}/m_{\text{sol}}$  constant. In the left panel  $m_{\text{atm}} = 10^{-4} \text{ eV}$ , while in the right panel  $m_{\text{atm}} = 10 \text{ eV}$ . One can see how the allowed region shrinks considerably, and almost disappears for these extreme values. This is one way to show the ‘leptogenesis conspiracy’ [45], that means how, order-of-magnitude-wise, the measured atmospheric and solar neutrino mass scales are optimal for leptogenesis to be successful. It should be noticed that for  $m_{\text{atm}} = 10 \text{ eV}$ , even though the lower bound on  $M_1$  is much lower, the density of points in the allowed region is very low since they correspond to a very fine-tuned situation where  $\tilde{m}_1 \ll m_{\text{atm}}$ .

In Fig. 2 we show the bounds for particular choices of the orthogonal matrix: in the

left panel for  $\Omega = R_{13}$ , corresponding to  $\omega_{21} = \omega_{32} = 0$ , and in the right panel for the effective two RH neutrino case obtained in the limit  $M_3/10^{14} \text{ GeV} \gg 1$  and corresponding to an orthogonal matrix with  $\omega_{21} = \omega_{32} = 1$ . In the first case, one can see how the bounds do not change compared to the general case, showing that this is the choice saturating the bounds, a well-known result [4]. Notice that for  $\Omega = R_{13}$  there is no dependence of the bounds on the light neutrino mass scheme, normal or inverted, and therefore, in vanilla leptogenesis, normal or inverted schemes produce the same bounds [4]. On the other hand, in the second case the lower bound on  $M_1$  becomes more stringent [41], especially in the case of inverted hierarchy. Indeed, in the vanilla case, for the same choice of the orthogonal matrix, the final asymmetry in an inverted scheme can be only less than in a normal scheme, or at most equal in the special case  $\Omega = R_{13}$ , as discussed analytically in [5]. This result is easy to understand qualitatively: the dominant term in the  $CP$  asymmetry is suppressed when the neutrino masses increase, either when  $m_1$  increases, or switching from normal to inverted hierarchy since in this case  $m_2$  gets higher.

In the next sections we will relax the assumptions of vanilla leptogenesis, studying how the leptogenesis bounds change accordingly. In most cases the effect of the assumptions on the bounds is independent of each other and therefore they can be studied individually. However, in a few cases the interplay of different effects can yield interesting interferences. For example, going beyond the hierarchical limit one has also to consider the contribution of the heavier RH neutrinos to the final asymmetry and to the washout.

## 4 Extra-term in the total $CP$ asymmetry

In this Section we relax the assumption  $M_2 = M_3$  defining vanilla leptogenesis, studying the effect on the bounds of the term proportional to  $\Delta\varepsilon_1(M_1, m_1, \Omega)$  in the Eq. (41), and comparing our results with those obtained in [24]. This effect clearly saturates to a maximum when  $M_3/M_2 \gg 1$  and in the plots we fixed  $M_3/M_2 = 100$ .

From the Eq. (41) it can be noticed that this effect acts independently of flavor effects and can be even dominant when the parameters are properly tuned. In particular this extra-term is able, although with quite a strong fine-tuning, to relax the lower bound on  $M_1$ . A separate analysis is fully justified since there is no interference between the two effects. In the 6 panels of Fig. 3, we show the crucial role played by the parameter  $\omega_{32}$  [5] in enhancing the extra-term in the total  $CP$  asymmetry (cf. Eq. (40)). This relaxes the mass bounds in a remarkable way if  $|\omega_{32}| \gg 1$  since the  $CP$  asymmetry enhancement is not counterbalanced by an increase of the washout that is driven by  $K_1$  and that is independent of  $\omega_{32}$ . It can be seen in the top right panel that when  $\omega_{32} = 0$  the bounds



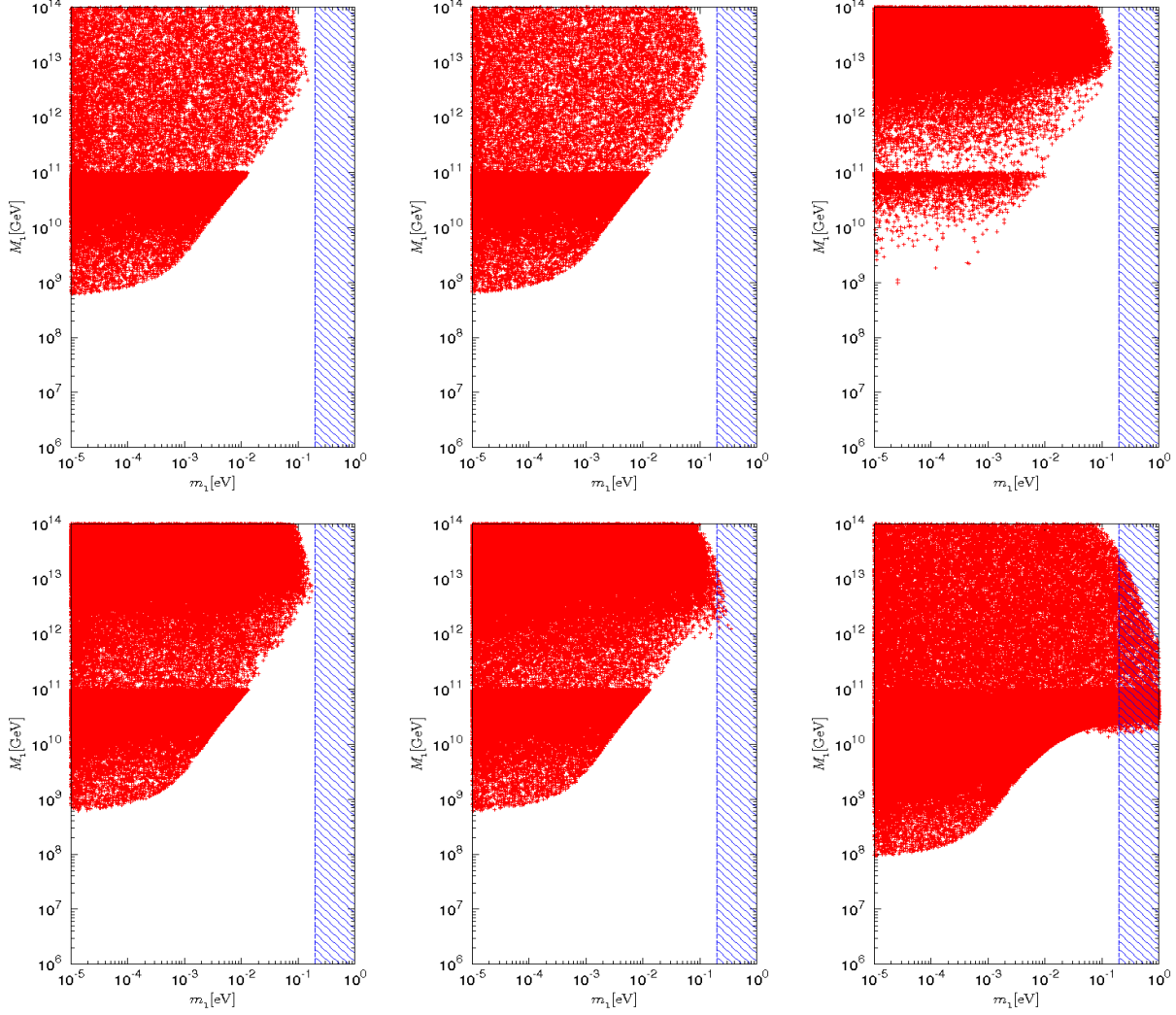


Figure 3: Effect of the extra term [cf. Eqs. (40) and (41)] in  $\varepsilon_1$  on the neutrino mass bounds. In all panels  $M_3 = 100 M_2$  and  $M_2 = 3 M_1$ , except in the top center panel where  $M_2 = 10 M_1$ . Top left and top center panel: all three  $|\omega_{ij}| \leq 1$ ; top right panel:  $|\omega_{32}| = 0$  while  $|\omega_{21}|, |\omega_{31}| \leq 10$ ; bottom left panel:  $|\omega_{21}|, |\omega_{32}| \leq 1, |\omega_{31}| \leq 10$ ; bottom center panel:  $|\omega_{31}|, |\omega_{32}| \leq 1, |\omega_{21}| \leq 10$ ; bottom right panel:  $|\omega_{21}|, |\omega_{31}| \leq 1, |\omega_{32}| \leq 10$ .

are almost unchanged, even though we allowed  $|\omega_{21}|, |\omega_{31}| \leq 10$ .

Notice that  $\Delta\varepsilon_1$  increases with the neutrino masses, contrarily to  $\bar{\varepsilon}_1$ . This is the reason why it tends to relax the upper bound on  $m_1$ . It also tends to be higher for inverted schemes compared to normal schemes, even though the bounds are saturated for a choice of the parameters where there is no dependence on  $m_2$  so that inverted and normal schemes give the same results.

The results of the panels can be easily understood analytically using Eqs. (40) and (41). For example, since  $\xi(x) \simeq 1 + 5/(9x)$  when  $x \gg 1$ , the extra-term is suppressed like  $(M_1/M_2)^2$ . It should be also noticed that the extra-term vanishes exactly in the limit of two effective RH neutrinos, obtained for  $M_3/10^{14} \text{ GeV} \rightarrow \infty$ .

In conclusion, the possibility to exploit the extra-term  $\propto \Delta\varepsilon_1(M_1, m_1, \Omega)$  to relax the lower bound on  $M_1$  relies on models where  $|\omega_{32}| \gtrsim 0.2 (M_2/M_1)^2$ . Therefore, already for  $M_2 \gtrsim 3 M_1$ , quite a high level of fine tuning is required. Concerning the upper bound on  $m_1$  the conditions are less stringent:  $|\omega_{32}| \gtrsim 0.2 (M_2/M_1)^2$  and/or  $|\omega_{21}| \gtrsim (M_2/M_1)^2$ , such that one has to impose, more conservatively,  $M_2 \gtrsim 10 M_1$ . We will see in the next Section that flavor effects have a bigger impact in relaxing the bounds compared to the vanilla scenario.

## 5 Adding flavor to vanilla

Relaxing only the second assumption defining vanilla leptogenesis, one has

$$\begin{aligned} N_{B-L}^f &= \sum_{\alpha} \varepsilon_{1\alpha} \kappa_{1\alpha}^f \\ &\simeq N_{\text{fl}} \bar{\varepsilon}_1(M_1, m_1, \omega_{21}, \omega_{31}) \kappa_1^f(M_1, m_1, K_1) + \frac{1}{2} \Delta P_{1\alpha}(M_1, m_1, \Omega, U) [\kappa_{1\alpha}^f - \kappa_{1\beta}^f]. \end{aligned} \quad (50)$$

From Eq. (13), in the HL, one finds [6]  $\varepsilon_{1\alpha} = \bar{\varepsilon}_{1\alpha} + \Delta\varepsilon_{1\alpha}$ , where

$$\bar{\varepsilon}_{1\alpha} \equiv \frac{3}{16 \pi (h^\dagger h)_{11}} \sum_{j \neq 1} \frac{1}{\sqrt{x_j}} \text{Im} [h_{\alpha 1}^* h_{\alpha j} (h^\dagger h)_{1j}] \quad (51)$$

and

$$\Delta\varepsilon_{1\alpha} \equiv \frac{1}{8 \pi (h^\dagger h)_{11}} \sum_{j \neq 1} \frac{1}{x_j} \text{Im} [h_{\alpha 1}^* h_{\alpha j} (h^\dagger h)_{j1}]. \quad (52)$$

Taking advantage of the orthogonal parametrization (cf. Eq. (29)) and defining  $r_{1\alpha} \equiv \varepsilon_{1\alpha}/\bar{\varepsilon}(M_1) = \bar{r}_{1\alpha} + \Delta r_{1\alpha}$ , one has

$$\bar{r}_{1\alpha} = - \sum_{h,l} \frac{m_l \sqrt{\tilde{m}_l m_h}}{\tilde{m}_1 m_{\text{atm}}} \text{Im}[U_{\alpha h} U_{\alpha l}^* \Omega_{h1} \Omega_{l1}] \quad (53)$$

and

$$\Delta r_{1\alpha} = \frac{2}{3} \sum_{j,h,l,k} \frac{M_1}{M_j} \frac{m_h \sqrt{m_l m_k}}{\tilde{m}_1 m_{\text{atm}}} \text{Im}[U_{\alpha l}^* U_{\alpha k} \Omega_{hj}^* \Omega_{l1}^* \Omega_{h1} \Omega_{kj}]. \quad (54)$$

The second term has been neglected in previous analyses but, as we will see, it can dominate under some conditions relaxing the leptogenesis bounds holding in the vanilla scenario. The most important difference between the two terms is that the first is upper bounded [11],

$$\bar{r}_{1\alpha} < \sqrt{P_{1\alpha}^0} m_3 / m_{\text{atm}}, \quad (55)$$

while the second is not. From this point of view the  $\Delta \varepsilon_{1\alpha}$  term is analogous to the extra term in the total  $CP$  asymmetry but, as we will see, it affects the bounds in a more relevant way.

The analytical expressions for the  $\kappa_{1\alpha}^f$ , generalizing those for  $\kappa_1^f$ , can be found in [6]. The generalization of the expression (47) becomes

$$M_1 = \frac{\bar{M}}{\sum_{\alpha} \kappa_{1\alpha}^f(M_1, m_1, \Omega, U) r_{1\alpha}(m_1, \Omega, U)}. \quad (56)$$

In the fully flavored regime this gives rise to a lower bound on  $M_1$  that always falls in the two-flavor regime with negligible washout from  $\Delta L = 2$  processes. Therefore, this can be expressed like

$$M_1 = \frac{\bar{M}}{r_{1\tau} \kappa_{1\tau}^f + r_{1,e+\mu} \kappa_{1,e+\mu}^f} \simeq \frac{\bar{M}}{N_{\text{fl}} \kappa_1^f(K_1) + \frac{1}{2} [\Delta P_{1\tau} / \bar{\varepsilon}(M_1)] [\kappa_{1\tau}^f - \kappa_{1,e+\mu}^f]}. \quad (57)$$

From the approximate expression, one can see once more that the lower bound, can be relaxed compared to the unflavored case only if there is some washout, otherwise  $N_{\text{fl}} = 1$  and  $\kappa_{1\tau}^f - \kappa_{1,e+\mu}^f = 0$ . This implies  $K_1 \gtrsim 1$ . In the limit of no washout, for  $K_1 \ll 1$ , one recovers the usual lower bound  $M_1 > \bar{M}$  in the case of initial thermal abundance. In the strong washout a big relaxation is possible only in the one-flavor dominance case, where one of the projectors  $P_{1\alpha}^0 \ll P_{1\beta}^0$ , otherwise close to the democratic case, where  $P_{1\alpha}^0 \simeq P_{1\beta}^0$ , the difference  $[\kappa_{1\tau}^f - \kappa_{1,e+\mu}^f]$  tends to suppress the final asymmetry.

## 5.1 Lower bound on $M_1$

In Fig. 4 we show the allowed region in the  $(K_1, M_1)$  plane for  $m_1 = 0$ . The plots are obtained scanning the seven free parameters,  $M_1$  and the 6 parameters in  $\Omega$ , showing only the points where  $\eta_B \geq \eta_B^{\text{CMB}}$  at  $3\sigma$ . This is equivalent to search for the points where  $M_1$  is larger than the right-hand side of the Eq. (56) with  $\bar{M} \simeq 5.7 \times 10^8 \text{ GeV}$ . In this

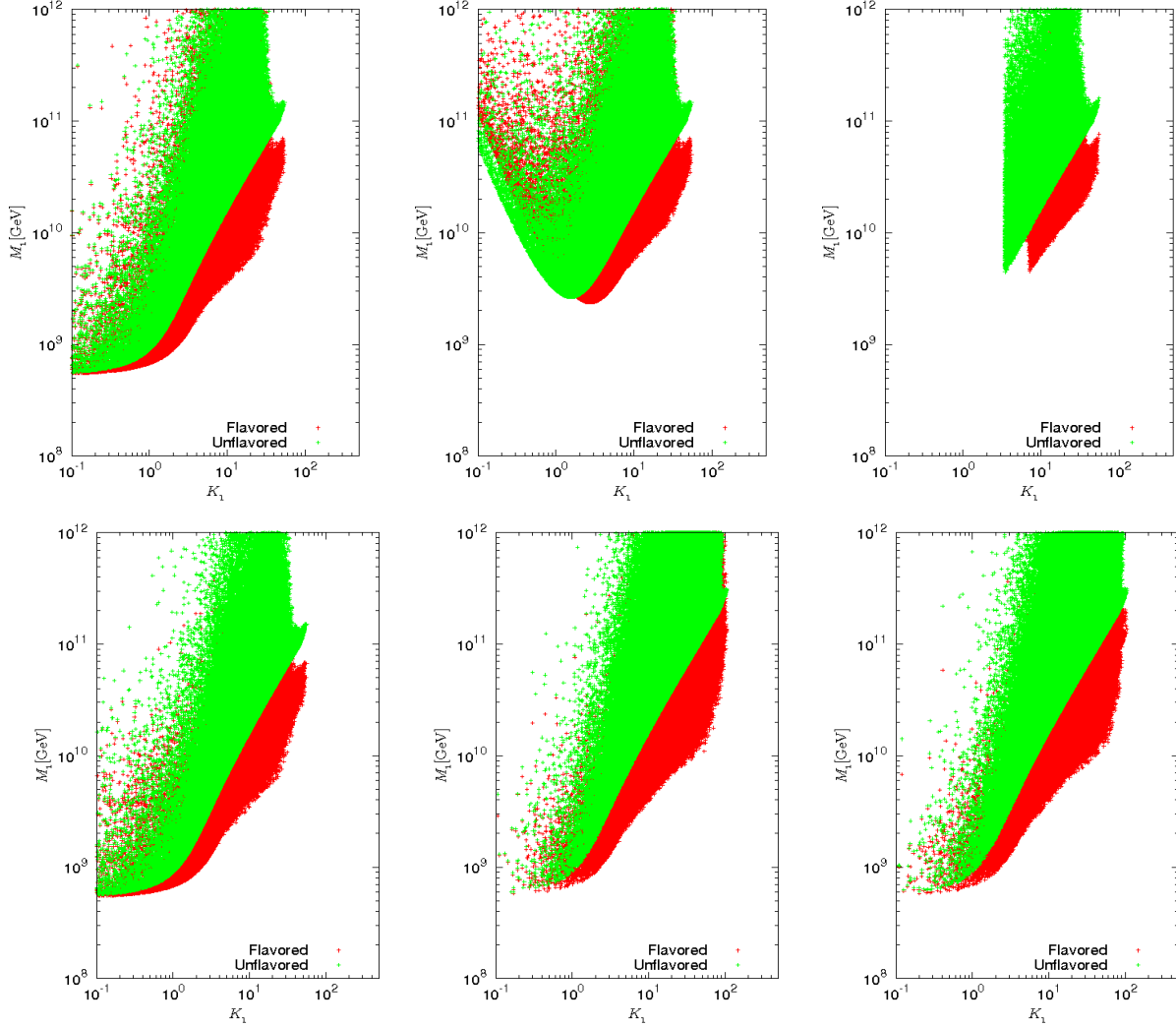


Figure 4: Lower bound on  $M_1$  versus  $K_1$  for  $m_1 = 0$  and imposing  $|\omega_{ij}| < 1$ . We show the results obtained in the fully flavored regime (red points) comparing them with those obtained when they are neglected (green points). Top-left panel: thermal initial  $N_1$ -abundance ( $N_{N_1}^{\text{in}} = 1$ ). Top-center panel: vanishing initial  $N_1$ -abundance ( $N_{N_1}^{\text{in}} = 0$ ). Top-right panel: points falling in the strong washout regime where the final asymmetry depends on the initial  $N_1$ -abundance to a level less than 10%. All bottom panels assume a thermal initial  $N_1$ -abundance. Bottom-left panel: like top-left but removing all points that violate the condition (36). Bottom-center and right panel: inverted hierarchy keeping or removing points violating the condition (36) respectively.

subsection we are imposing  $|\omega_{ij}| \leq 1$ , implying an upper bound on  $K_1$ . We will study in Section 5.3 the effects of turning on large values of  $|\omega_{ij}|$ .

In the plots the red region is the additional part of the allowed region due to flavor effects within the fully flavored regime while the green region is what one obtains within vanilla leptogenesis neglecting flavor effects. In the top-left panel the final asymmetry has been calculated for an initial thermal  $N_1$ -abundance, while in the top-middle panel for an initial vanishing  $N_1$ -abundance. One can see again that flavor effects can relax the lower bound only in the presence of washout, that means when  $K_1 \gtrsim 1$  and the amount of the relaxation increases with  $K_1$ . Essentially the lower bound we find coincides with the lower bound found analytically in [6] that corresponds to neglect  $\Delta r_{1\alpha}$  and maximizing  $\bar{r}_{1\alpha}$  and  $\kappa_{1\alpha}^f$  in the Eq. (56) in the case of one flavor dominance. In [6] the lower bound was numerically calculated only for a particular case,  $\Omega = R_{13}$ , and just a small relaxation was found for vanishing  $m_1$ . Here, allowing for  $\omega_{21} \neq 0$ , we find a large relaxation also for vanishing  $m_1$ . In the top-right panel, we selected only the points for which there is independence of the initial conditions, more exactly those for which there is a difference to a level less than 10% between thermal and vanishing initial  $N_1$ -abundance. This generalizes the definition of strong washout regime when flavor effects are taken into account. The critical value of  $K_1$  increases from  $\sim 3$  in the unflavored case to  $\sim 7$  in the flavored case.

In the bottom left panel we finally show only the points that further satisfy the condition of validity of the classic kinetic equations in the fully flavored regime (cf. Eq. (36)), and one can see how there are no differences between the unflavored and the fully flavored regime since these arise for larger  $K_1$  values.

In the bottom center and right panels we show the results for inverted hierarchy without imposing the condition of validity and imposing it, respectively. One can see that the situation is not very different from the normal hierarchy case. Slightly larger values of  $K_1$  are allowed, up to about  $2 \times K_{\text{atm}} \simeq 93$ . This implies that the relaxation of the lower bound on  $M_1$  can be as large as one order of magnitude for the maximal allowed value of  $K_1$ . Notice that these points still satisfy the condition of validity (36).

In Fig. 5 we consider two special cases for the orthogonal matrix when  $m_1 = 0$ . In the left panel  $\Omega = R_{13}$  (i.e.  $\omega_{21} = \omega_{32} = 0$ ). In this case it is easy to show [6] that  $\Delta P_{1\alpha} = 0$  and therefore in the Eq. (50) only the first term survives and all flavor effects reduce to an enhancement of the final asymmetry compared to vanilla leptogenesis given just by  $N_f \sim 2$ . In the right panel we consider the case of very large  $M_3 \gg 10^{14}$  GeV to be compared with the right panel of Fig. 2 in the unflavored case. One can see that this time inverted hierarchy (green and purple areas) is not so suppressed compared to normal

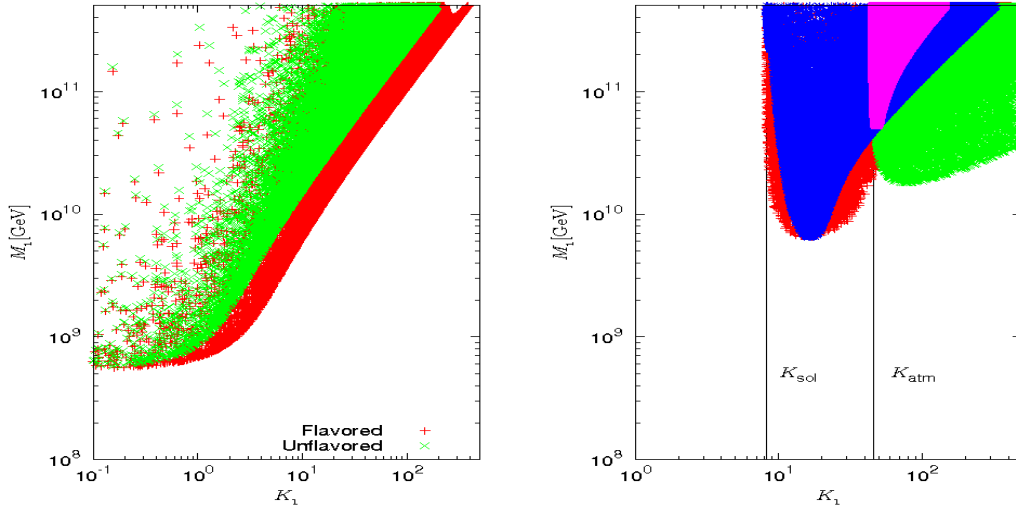


Figure 5: Lower bound on  $M_1$  versus  $K_1$  for  $\Omega = R_{13}$  (left) and for  $M_3 \gg 10^{14}$  GeV (right). In the right panel the red and blue regions correspond to normal hierarchy and the purple and the green to inverted hierarchy. The blue and purple regions are obtained switching off the PMNS phases.

hierarchy (red and blue areas) as in the unflavored case. This is due to the presence of the PMNS phases that give a further contribution to the asymmetry. Indeed when phases are switched off (purple and blue areas) again the allowed region for inverted hierarchy is strongly reduced compared to normal hierarchy, similarly, though to a minor extent, to what happened in the unflavored case. In this specific case  $M_3 \gg 10^{14}$  GeV, the effect of phases has been recently studied in [46]. The fact that PMNS phases can give a dominant contribution to the final asymmetry was first noticed in the case  $\Omega = R_{13}$  and  $m_1 \neq 0$  in [6].

## 5.2 Upper bound on $m_1$

In this subsection we allow  $m_1 \neq 0$ , investigating how the upper bound on  $m_1$  and its dependence on  $M_1$  changes when flavor effects are included. For this purpose, we show plots in the  $(M_1, m_1)$  plane. As in the last subsection, we impose the condition  $|\omega_{ij}| \leq 1$ .

In all figures we distinguish three different kinds of points: those characterized by a strong one-flavor dominance for which  $P_{1\tau}^0 < 0.1$  or  $P_{1e}^0 + P_{1\mu}^0 < 0.1$  (red crosses), those characterized by a mild one-flavor dominance for which  $0.1 < P_{1\tau}^0 < 0.45$  or  $0.1 < P_{1e}^0 + P_{1\mu}^0 < 0.45$  (green x) and finally those for which a democratic scenario is realized

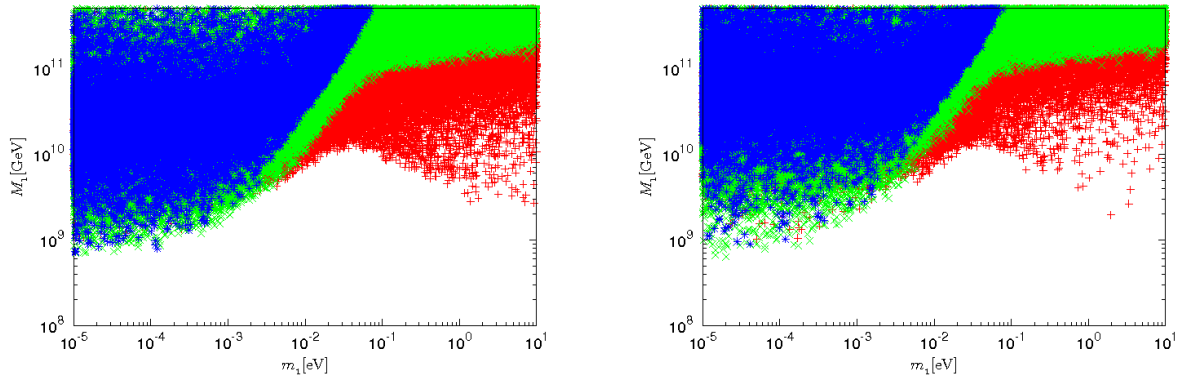


Figure 6:  $M_1$  vs.  $m_1$  for normal (left panel) and inverted (right panel) hierarchy. The red straight crosses denote a projector  $P_{1\tau}^0 < 0.1$  or  $P_{1e}^0 + P_{1\mu}^0 < 0.1$ , the green x's  $0.1 < P_{1\tau}^0 < 0.45$  or  $0.1 < P_{1e}^0 + P_{1\mu}^0 < 0.45$  and the blue stars  $0.45 < P_{1\tau}^0 < 0.5$  or  $0.45 < P_{1e}^0 + P_{1\mu}^0 < 0.5$ .

such that  $0.45 < P_{1\tau}^0, P_{1e}^0 + P_{1\mu}^0 < 0.55$  (blue stars). This will make possible to understand under which circumstances the upper bound on  $m_1$  can be evaded when flavor effects are taken into account.

In Fig. 6 the results are shown both for normal (left panel) and inverted (right panel) hierarchy and have been obtained using the approximation  $C = I$ . One can see that there is no upper bound on  $m_1$ , as first pointed out in [11]. The evasion of the bounds occurs in a one-flavor dominance, as expected. Note that the results have been obtained without imposing the condition of validity of the fully flavored regime Eq. (36). In the case of inverted hierarchy (right panel) the bounds do not change significantly.

In Fig. 7 we consider the special case  $\Omega = R_{13}$ , corresponding to  $\omega_{21} = \omega_{32} = 0$  in the Eq. (32). The number of free parameters gets therefore reduced to 6 (one of the PMNS phases,  $\Phi_2$ , is irrelevant in this model). One can see that the bounds are very similar to the general case, just slightly more stringent at large  $m_1$ . Therefore, the special case  $\Omega = R_{13}$  gives an approximate condition for the saturation of the bounds in the  $(m_1, M_1)$  plane. The phases in the PMNS matrix can play a crucial role in the fully flavored regime. This was first emphasized in [10] and then analyzed in more detail in [14, 6]. Here we want to show the effects of the PMNS phases on the lower bound found in the previous figures comparing the previous results with those obtained when the PMNS phases are turned off. The result for a general  $\Omega$  matrix is not shown because it is given precisely by Fig. 6. There are indeed enough phases present in the  $\Omega$  matrix in this case to realize a strong one-flavor dominance and to saturate the general lower bound even though the

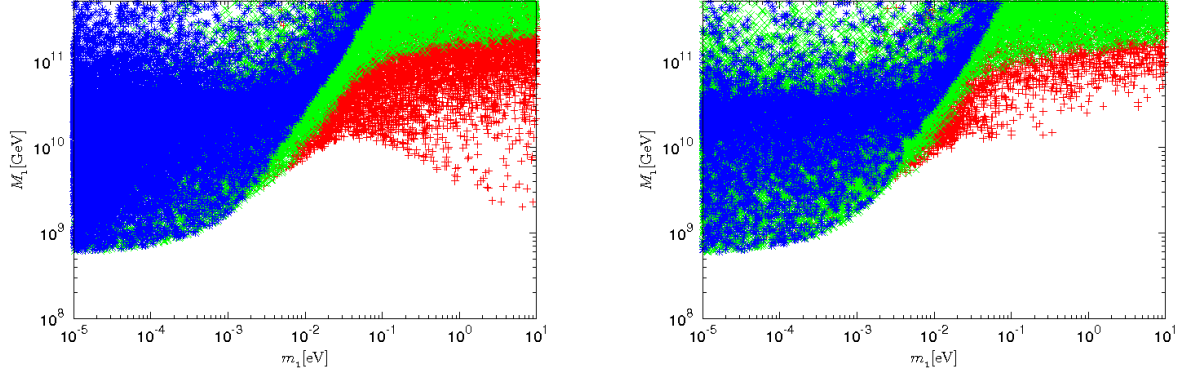


Figure 7: Same as in Fig. 6 but for the special case  $\Omega = R_{13}$ .

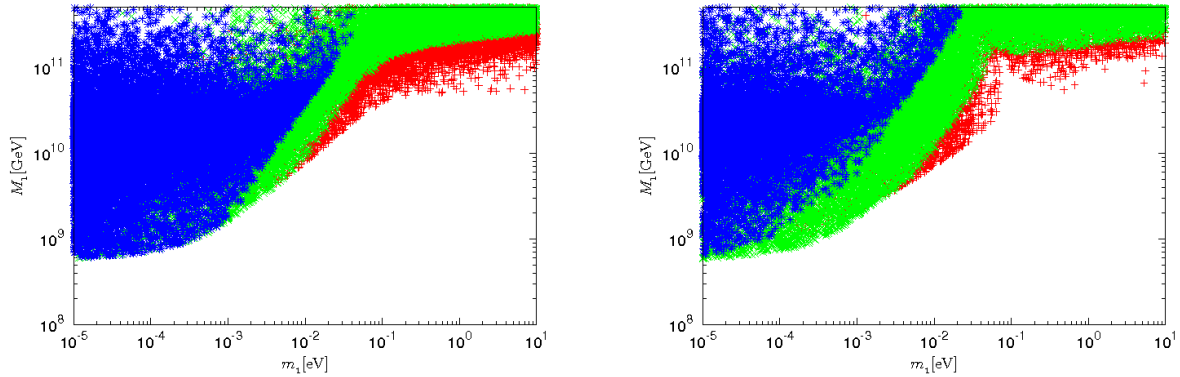


Figure 8: Same as Fig. 6, for  $\Omega = R_{13}$  with all PMNS phases turned off.

PMNS phases are set to zero. The situation is different when one considers special cases like  $\Omega = R_{13}$  as first found in [6]. The result is shown in Fig. 8 and comparing with Fig. 7 one can see clearly that the PMNS phases are responsible for the saturation of the bounds at large  $m_1$ . The reason is that there is in this case only one phase in the  $\Omega$  matrix, and this is not enough to fulfill the conditions for the saturation of the lower bound. Therefore, the Majorana phase  $\Phi_1$  and the Dirac phase  $\delta$  play a crucial role in this case analogously to the case  $M_3 \gg 10^{14}$  GeV for inverted hierarchy, as seen in the previous subsection and recently pointed out in [46].

Let us now discuss the consequence of imposing the condition of validity of the fully flavored regime, Eq. (36). The result is shown in the left panel of Fig. 9, to be compared with Fig. 6 where the same parameters were varied but all points were kept. One notices clearly that many points at large  $m_1$  disappear and an upper bound on  $m_1$ , given by  $m_1 \lesssim 0.15$  eV, appears again and is comparable to the upper bound holding in the



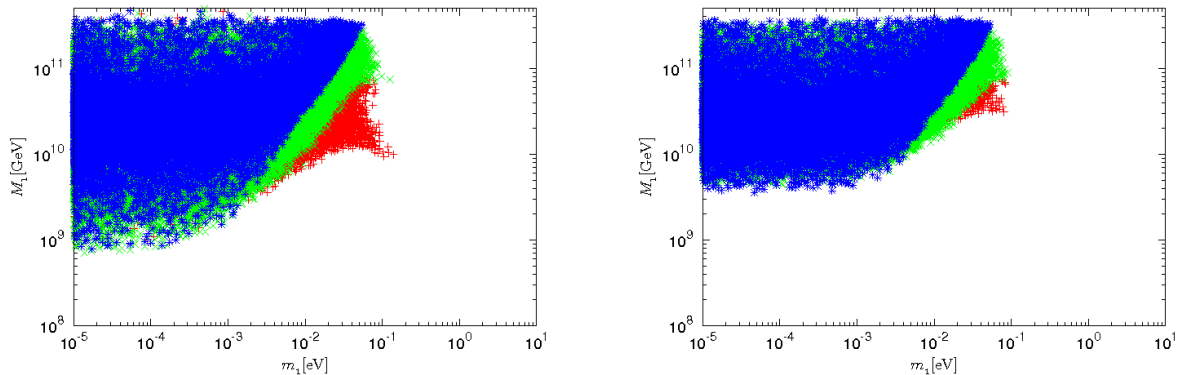


Figure 9: Same as Fig. 6, imposing the condition of validity of the fully flavored regime (left panel) and the strong washout condition (right panel).

unflavored regime,  $m_i \lesssim 0.12$  eV. In the case of inverted hierarchy similar results apply. However, it should be clarified that  $m_1 \lesssim 0.15$  eV is not an upper bound on the neutrino masses but a limit of validity of the fully flavored regime. One should therefore solve more general kinetic density matrix equations in order to describe the intermediate regime and to see whether there is or not an upper bound on neutrino masses. In the right panel of the same figure, we also imposed the strong washout regime condition and one can see that the allowed region gets further reduced and the upper bound on  $m_1$  even more stringent,  $m_1 \lesssim 0.10$  eV.

So far all results have been obtained making use of the approximation  $C = I$ . In the upper panels of Fig. 10, left for normal hierarchy and right for inverted hierarchy, we show the results without taking into account the Higgs asymmetry solving the Eq.'s (24) neglecting  $C^H$  in  $C$  that reduces to  $C^l$  given by the expression (25). One can see that the upper bound on  $m_1$  gets relaxed when  $C^H$  is neglected. In the bottom panels we used the Eq. (27) for  $C$  and one can see that the results agree very well with those obtained when we used the approximation  $C = I$ . Therefore, we will continue to use this approximation in the following analysis.

A particularly interesting case to be discussed is when all the high-energy phases are switched off, i.e. imposing the  $\Omega$  matrix to be real. In this case the PMNS phases act as the only source of  $CP$  violation responsible for the explanation of the observed matter-antimatter asymmetry [10]. It is therefore interesting to understand whether there is an allowed region at all [6]. The results are shown in Fig. 11 for  $M_3 = M_2 = 3 M_1$ . We show both the results obtained when both Majorana and the Dirac phase are switched on (red points) and those obtained when only the Dirac phase is non-vanishing (green points) and

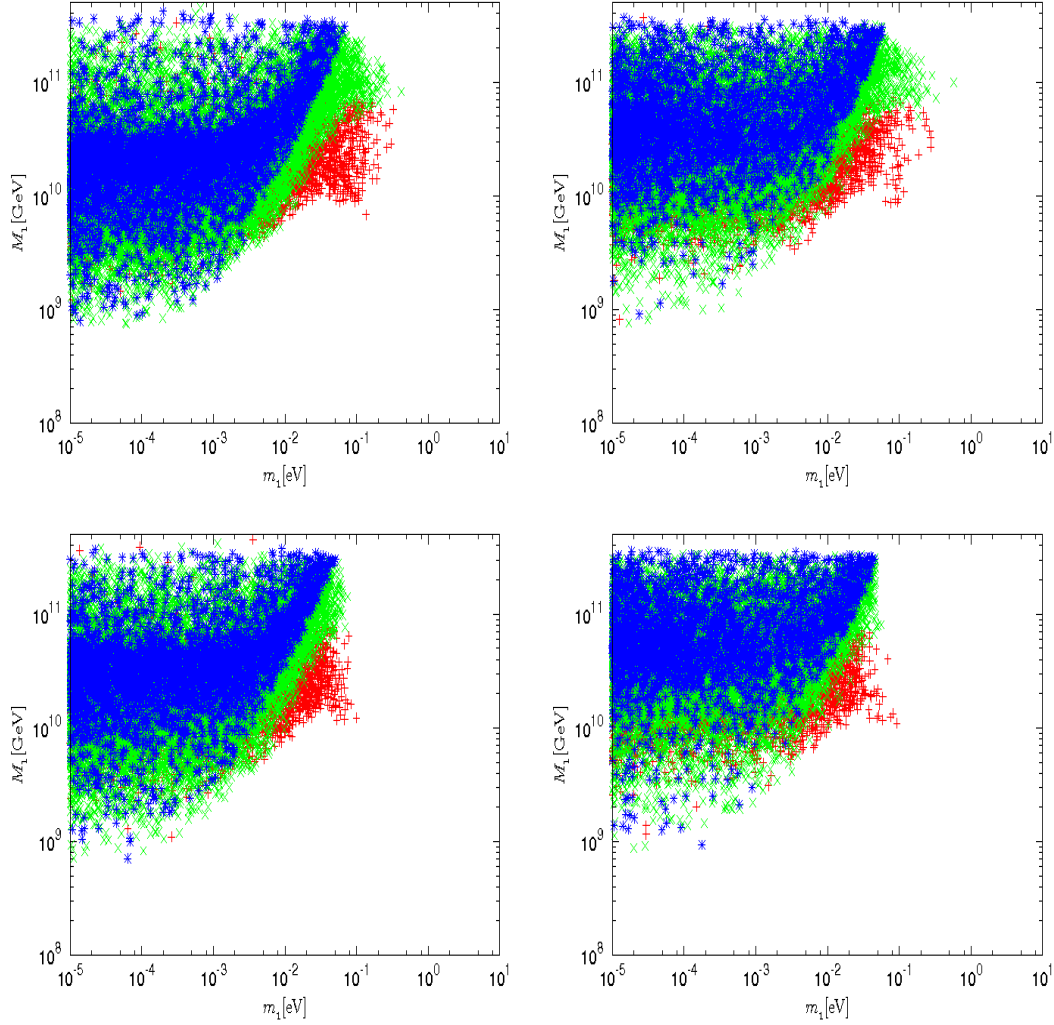


Figure 10: Check of the approximation  $C = I$ . In the upper panels we neglected the Higgs asymmetry solving the Eq.'s (24) with  $C^H = 0$ . In the bottom panels we solved the Eq.'s (24) with  $C$  given by the Eq. (27).

for  $\sin\theta_{13} = 0.2$ , the  $3\sigma$  experimental upper bound. This even more special case is the Dirac phase leptogenesis scenario [19]. The Dirac phase being the only phase that we can realistically measure in the near future in neutrino oscillation experiments, it is therefore particularly relevant to understand whether this testable source of  $CP$  violation can be also responsible for the observed matter-antimatter asymmetry.

The top-left panel is for normal hierarchy while the top-right is for inverted hierarchy. One can notice that in this last case the lower bound on  $M_1$  tends to infinite for vanishing  $m_1$ , meaning that the final asymmetry tends to vanish<sup>1</sup>. In both cases there is an upper bound on  $m_1$ , as first discussed in [17]. In the bottom-left panel we impose the condition of validity of the fully flavored regime given by the Eq. (36) and one can see that the allowed region gets reduced in a relevant way. Imposing even the strong washout regime condition (i.e. independence of the initial conditions) one can see that the allowed regions gets further reduced and it practically disappears for the case of Dirac phase leptogenesis, confirming, more generally, what was found in [19].

### 5.3 Effect of large $|\omega_{ij}|$ values

So far, we imposed the restriction  $|\omega_{ij}| \leq 1$ . In this subsection we relax this restriction studying the effect of allowing  $|\omega_{ij}|$  as large as 10 on the bounds. The main effect is that the extra-term  $\Delta\varepsilon_{1\alpha}$  in the flavored  $CP$  asymmetries (cf. Eq. (52)) can become dominant. The upper bound Eq. (55) does not apply to this term. Since this term is suppressed like  $M_1/M_2$  the dominance is possible for a mild hierarchical spectrum, such that  $M_2/M_1 < \mathcal{O}(100)$ . In any case notice that its dominance applies under conditions that are much less restrictive than those found for the dominance of  $\Delta\varepsilon_1$ , that is suppressed like  $(M_1/M_2)^2$  and that cancels when  $M_2 = M_3$ .

In Fig. 12 we show the allowed region in the plane  $(K_1, M_1)$  for  $m_1 = 0$  and for  $M_3 = M_2$  so that  $\Delta\varepsilon_1$  does not give any contribution. The results have to be compared with those in Fig. 4. The maximum effect is obtained again, like for  $\Delta\varepsilon_1$ , when  $\omega_{32}$  is large. In the top panels only  $|\omega_{32}|$  is allowed to be as large as 10, while  $|\omega_{21}|, |\omega_{31}| \lesssim 1$ . In the top-left panel and in the top-center panel, for normal and inverted hierarchy respectively and for  $M_2 = 3M_1$ . One can see how the lower bound on  $M_1$  gets relaxed of one order of magnitude so that it can be as low as  $10^8$  GeV. Analogous relaxation applies to the lower bound on the reheat temperature  $T_{\text{reh}}$ . Notice that in the limit of no washout, for  $K_1 \rightarrow 0$ , the usual unflavored lower bound is recovered. In the top-right panel  $M_2 = 30M_1$ , such that the extra-term  $\Delta\varepsilon_{1\alpha}$  is suppressed enough not to be able to relax the lowest bound

---

<sup>1</sup>Similar results have been recently obtained in [47].

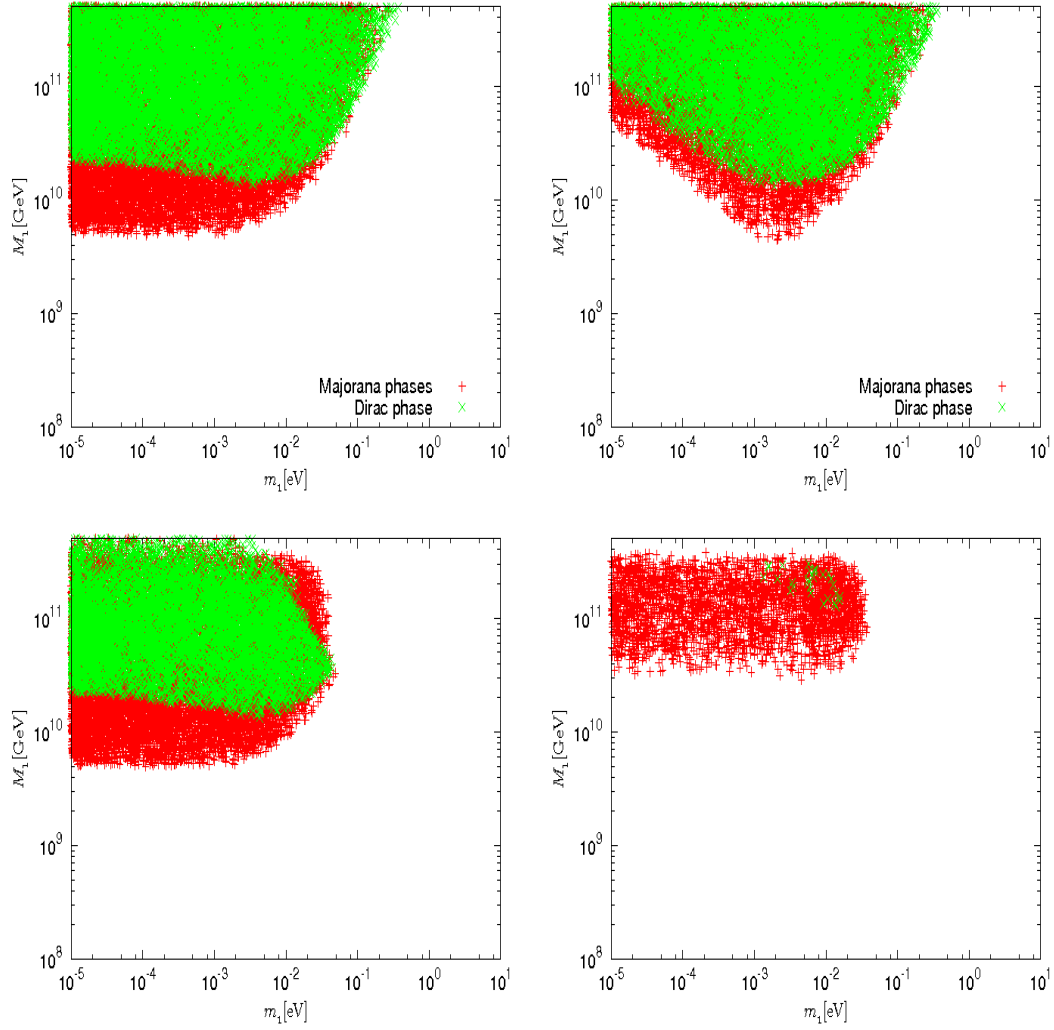


Figure 11: Leptogenesis only with Majorana phases (red points) and only with Dirac phase (green points). Top-left and top right panel: allowed region in the plane  $(m_1, M_1)$  for normal hierarchy and inverted hierarchy respectively. Bottom panels: the same as top-left but imposing the condition Eq. (36) (left) and the strong washout condition as well (right panel).

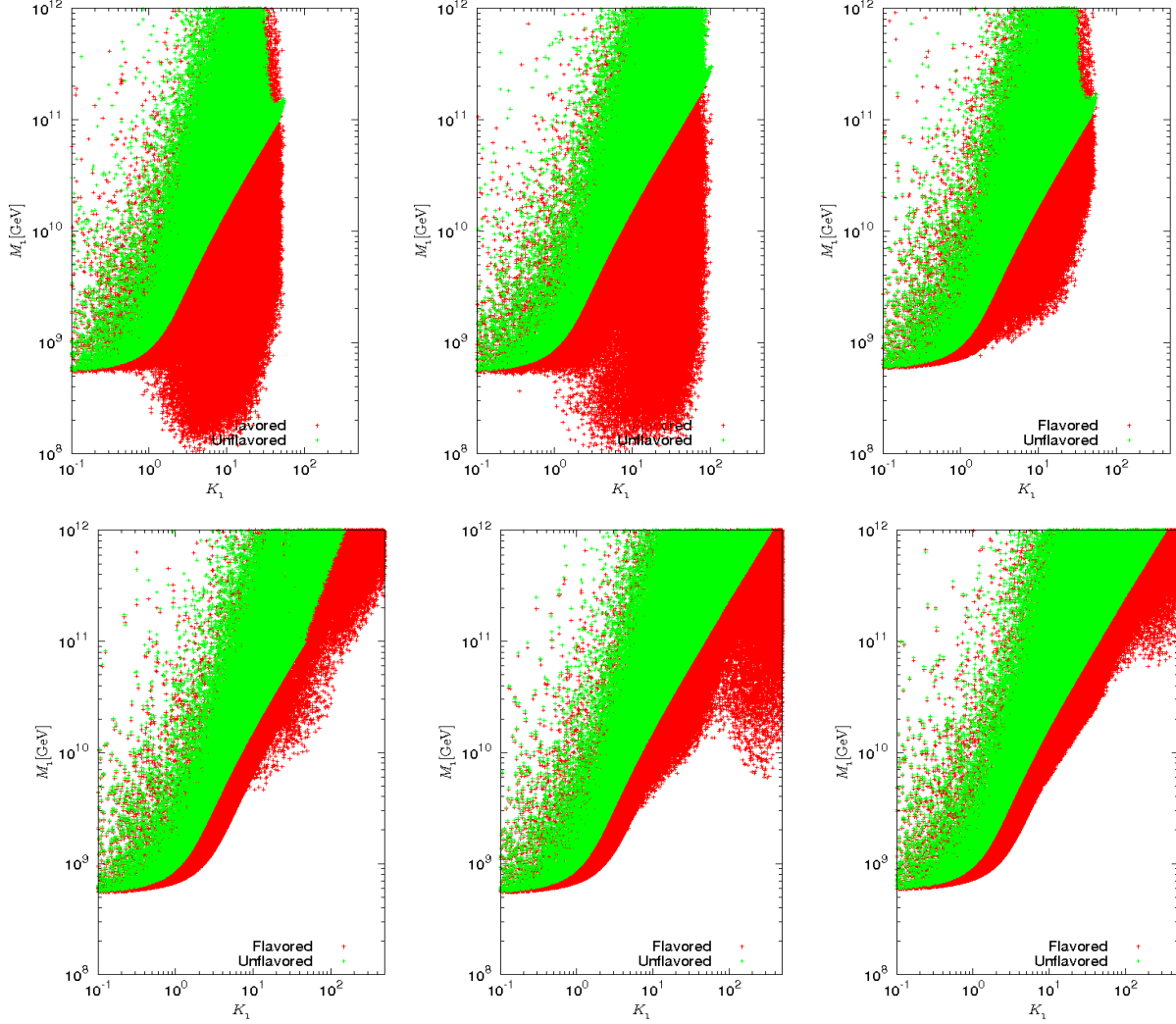


Figure 12: Lower bound on  $M_1$  versus  $K_1$  for  $m_1 = 0$ . The results are compared when flavor effects are neglected (green points) and when they are taken into account (red points) while all have been obtained for a thermal initial  $N_1$ -abundance ( $N_{N_1}^{\text{in}} = 1$ ). Top panels:  $|\omega_{21}|, |\omega_{31}| \leq 1, |\omega_{32}| \leq 10$ ; Top left and center panels: normal and inverted hierarchy, respectively, and  $M_2 = M_3 = 3M_1$ ; Top right panel: normal hierarchy and  $M_2 = M_3 = 30M_1$ . Bottom panels:  $|\omega_{31}|, |\omega_{32}| \leq 1, |\omega_{21}| \leq 10$ ; Bottom left and center panels: normal and inverted hierarchy, respectively, and  $M_2 = M_3 = 3M_1$ ; Bottom right panel: inverted hierarchy and  $M_2 = M_3 = 30M_1$ .

on  $M_1$ . In the bottom panels we allowed  $|\omega_{21}|$  to be as large as 10 while  $|\omega_{31}|, |\omega_{32}| \lesssim 1$ . One can see that the effect is much more reduced since now  $\Delta\varepsilon_{1\alpha}$  increases but at the same time  $K_1$  and the washout increase as well.

## 6 On the validity of the $N_1$ -dominated scenario

In general, the final asymmetry receives a contribution from the decays of all 3 RH neutrinos:  $N_{B-L}^f = \sum_i N_{B-L}^f(N_i)$ . In this Section we want to find a condition that guarantees the validity of the bounds within the  $N_1$ -dominated scenario, where  $N_{B-L}^f \simeq N_{B-L}^f(N_1)$ .

If  $M_3 \gtrsim 10^{12}$  GeV, then the asymmetry produced from the heaviest RH neutrino decays occurs always in the unflavored regime. If moreover we impose  $M_3 \gg M_2$ , then it can be always safely neglected since the total  $CP$  asymmetry  $\varepsilon_3 \propto (M_{1,2}/M_3)^2$  is strongly suppressed and at the same time a strong washout from  $N_1$  and  $N_2$  is unavoidable [5].

On the other hand,  $\varepsilon_2$  is not necessarily suppressed. A condition that guarantees the possibility to neglect  $N_{B-L}^f(N_2)$  in the determination of the bounds is equivalent to impose

$$\eta_B(N_2) \equiv a_{\text{sph}} \frac{N_{B-L}^f(N_2)}{N_\gamma} \ll \eta_B^{\text{CMB}}. \quad (58)$$

From the Eq. (8) and using the orthogonal parametrization, the  $CP$  asymmetry  $\varepsilon_2$  can be recast as [5]

$$\varepsilon_2 = \bar{\varepsilon}(M_2) \left[ \beta_{23}(m_1, \Omega) + \frac{4}{3} \frac{M_1^2}{M_2^2} \ln \left( \frac{M_2}{M_1} - 1 \right) \beta_{21}(m_1, \Omega) \right], \quad (59)$$

where we defined

$$\beta_{ij}(m_1, \Omega) \equiv \frac{\text{Im}[\sum_h m_h \Omega_{hi}^* \Omega_{hj}]}{\tilde{m}_i m_{\text{atm}}}. \quad (60)$$

There are two special cases for which the  $N_1$ -dominated scenario is certainly valid. The first is to have  $\Omega = R_{13}$  (i.e.  $\omega_{21} = \omega_{32} = 0$ ), since in this case it is simple to see that  $\varepsilon_2 = 0$ . The second case is the limit  $M_3 \gg 10^{14}$  GeV. In this case  $\Omega$  is given by the Eq. (33) and it is easy to see that  $\varepsilon_2 = 0$ . This result can be understood considering that in this limit the heaviest RH neutrino decouples and so necessarily the interference term  $(m_D^\dagger m_D)_{23} \rightarrow 0$ .

The opposite case is for  $\Omega = R_{23}$ , since now one has  $\varepsilon_1 = 0$  while

$$\varepsilon_2 \leq \bar{\varepsilon}(M_2) \frac{m_3 - m_2}{m_{\text{atm}}} f(m_2, \tilde{m}_2), \quad (61)$$

the same maximum value holding for  $\bar{\varepsilon}_1$  (cf. Eq. (49)) but where  $(m_1, M_1, \tilde{m}_1)$  are replaced by  $(m_2, M_2, \tilde{m}_2)$ . Notice moreover that for  $\Omega = R_{23}$  one has  $m_1 \ll m_*$ , so that the asymmetry produced from  $N_2$ -decays is certainly not washed out by  $N_1$ -inverse decays. In this situation a  $N_2$ -dominated scenario is realized, with  $N_{B-L}^f \simeq N_{B-L}^f(N_2)$  and with no lower bound on  $M_1$  [5].

Between these two well-defined special cases, one has to take into account both a contribution  $N_{B-L}^f(N_1)$  from  $N_1$ -decays and a contribution  $N_{B-L}^f(N_2)$  from  $N_2$ -decays. For example, choosing  $\Omega = R_{12}$  one has

$$\varepsilon_2 = \frac{4}{3} \frac{M_1}{M_2} \varepsilon_1. \quad (62)$$

Assuming that  $M_2 \gtrsim 5 \times 10^{11}$  GeV, such that the asymmetry from  $N_2$ -decays is produced in the unflavored regime and that  $M_2 \gg M_1$ , one can see that even neglecting the washout from  $N_1$ -inverse processes the contribution  $N_{B-L}^f(N_2)$  from  $N_2$ -decays can be safely neglected in the determination of the bounds.

This example shows that if the first term in the Eq. (59)  $\propto \text{Im}[(m_D^\dagger m_D)_{23}]^2$  vanishes, then  $\eta_B(N_2)$  can be neglected in the determination of the bounds in the hierarchical limit where  $M_2 \gg M_1$ . Therefore, a condition  $\text{Im}[(m_D^\dagger m_D)_{23}]^2 = 0$  certainly guarantees the validity of the  $N_1$ -dominated scenario but is quite a restrictive one. However, this condition enlightens that an asymmetry generated from  $N_2$ -decays requires an interference of the heaviest RH neutrino  $N_3$  with  $N_2$ . Indeed, as we said, this condition is certainly verified in the limit  $M_3 \gg 10^{14}$  GeV, when the heaviest RH neutrino decouples and  $(m_D^\dagger m_D)_{23} = 0$ .

Now we want to see whether, starting from  $\Omega = R_{13}$ , one can turn on a rotation  $R_{12}$  ( $\omega_{21} \neq 0$ ) still having a negligible  $\eta_B(N_2)$ . Since both for  $\Omega = R_{13}$  and  $\Omega = R_{12}$  one has  $(m_D^\dagger m_D)_{23} = 0$ , one could naively think that this is still true for  $\Omega = R_{12} R_{13}$  and therefore that  $\omega_{32} = 0$  is a sufficient condition for the validity of the  $N_1$ -dominated scenario. However it is easy to check it is not true that  $(m_D^\dagger m_D)_{23} = 0$  and therefore it is not guaranteed that the asymmetry from  $N_2$ -decays can be neglected. This has to be done by inspection. Since we are assuming the hierarchical limit,  $M_2 \gtrsim 3 M_1$ , the calculation of  $N_{B-L}^f(N_2)$  factorizes in two terms

$$\eta_B(N_2) = \eta_B(N_2)|_{T \sim T_B(K_2)} \times w_1(T \sim M_1). \quad (63)$$

The first term is the asymmetry produced at  $T_B \simeq M_2/z_B(K_2)$  from  $N_2$ -decays, while the second term is the washout from  $N_1$ -inverse processes.

A precise calculation of  $w_1(T \sim M_1)$  has to take into account two types of flavor effects. If  $M_1 \lesssim 10^9$  GeV, then the asymmetry produced from  $N_2$ -decays is fully projected

on the three-flavor basis at the time when the asymmetry is washed out by  $N_1$ -inverse processes [49]. Assuming moreover that  $M_2 \gtrsim 5 \times 10^{11}$  GeV, so that the asymmetry from  $N_2$  decays is produced in the unflavored regime, the contribution to the final asymmetry from  $N_2$ -decays can be calculated as

$$N_{B-L}^f(N_2) = \varepsilon_2 \kappa(K_2) \sum_{\alpha} P_{2\alpha}^0 e^{-\frac{3\pi}{8} P_{1\alpha}^0 K_1}. \quad (64)$$

On the other hand, if  $M_2 \lesssim 5 \times 10^{11}$  GeV, then the asymmetry is produced in the fully flavored regime and

$$N_{B-L}^f(N_2) = \sum_{\alpha} \varepsilon_{2\alpha} \kappa(K_{2\alpha}) e^{-\frac{3\pi}{8} P_{1\alpha}^0 K_1}. \quad (65)$$

Notice, however, that since we are interested in finding the condition for the  $N_1$ -dominated scenario to hold, then  $M_1 \gtrsim 10^9$  GeV and at the time of the washout from  $N_1$ -inverse processes the asymmetry is projected on a two-flavor basis: the  $\tau$  flavor and an orthogonal combination of electron and muon flavors. In this situation  $N_1$ -inverse processes have the effect to further project the asymmetry stored in the  $e+\mu$  flavor on a two-flavor basis where one direction is determined by  $l_1$  and the other is the orthogonal component [12, 48]. The washout from  $N_1$ -inverse decays does not touch this orthogonal component and therefore, accounting for this effect, the value of the final asymmetry has to lie somewhere between the value of the asymmetry produced at  $T \sim T_B(K_2)$  and the value of the asymmetry calculated neglecting the effect of projection along  $l_1$ ,

$$N_{B-L}^f(N_2)|_{T \sim z_B(K_2)} \times w_1(T \sim M_1) \lesssim N_{B-L}^f(N_2) \lesssim N_{B-L}^f(N_2)|_{T \sim z_B(K_2)}. \quad (66)$$

As already mentioned, two special cases where the validity of the  $N_1$ -dominated scenario is guaranteed are  $M_3 \gg M_2 \gtrsim 10^{14}$  GeV and  $\Omega = R_{13}$ . In Fig. 13 we show the results obtained in a more general case. We allow  $\Omega = R_{12}(\omega_{21}) R_{13}(\omega_{31})$  where  $\omega_{21} \neq 0$  but still  $\omega_{32} = 0$ . In the left panels we show the results in the plane  $(M_2, \eta_B(N_2))$ . The final asymmetry is calculated both neglecting the washout (red points) and with the washout calculated in the two-flavor regime (green points) but neglecting the effect of projection of the asymmetry due to  $N_1$ -inverse processes: as we said an account of this effect should give a result that has to be somehow in between. One can see in the top-left panel that for  $M_2 \lesssim 10^{11-12}$  GeV the asymmetry produced by  $N_2$ -decays falls below the observed one indicated by the horizontal solid line. Here we are imposing  $\omega_{21} \leq 1$  and we are assuming the reheat temperature to be higher than  $\sim T_B(N_2) \sim M_2/z_B(K_2)$ . This result can be actually also translated into a condition on the reheat temperature given by  $T_{\text{reh}} \lesssim T_B(N_2) \sim M_2/z_B(K_2)$ , while  $M_2$  this time is free. The result is shown in the right



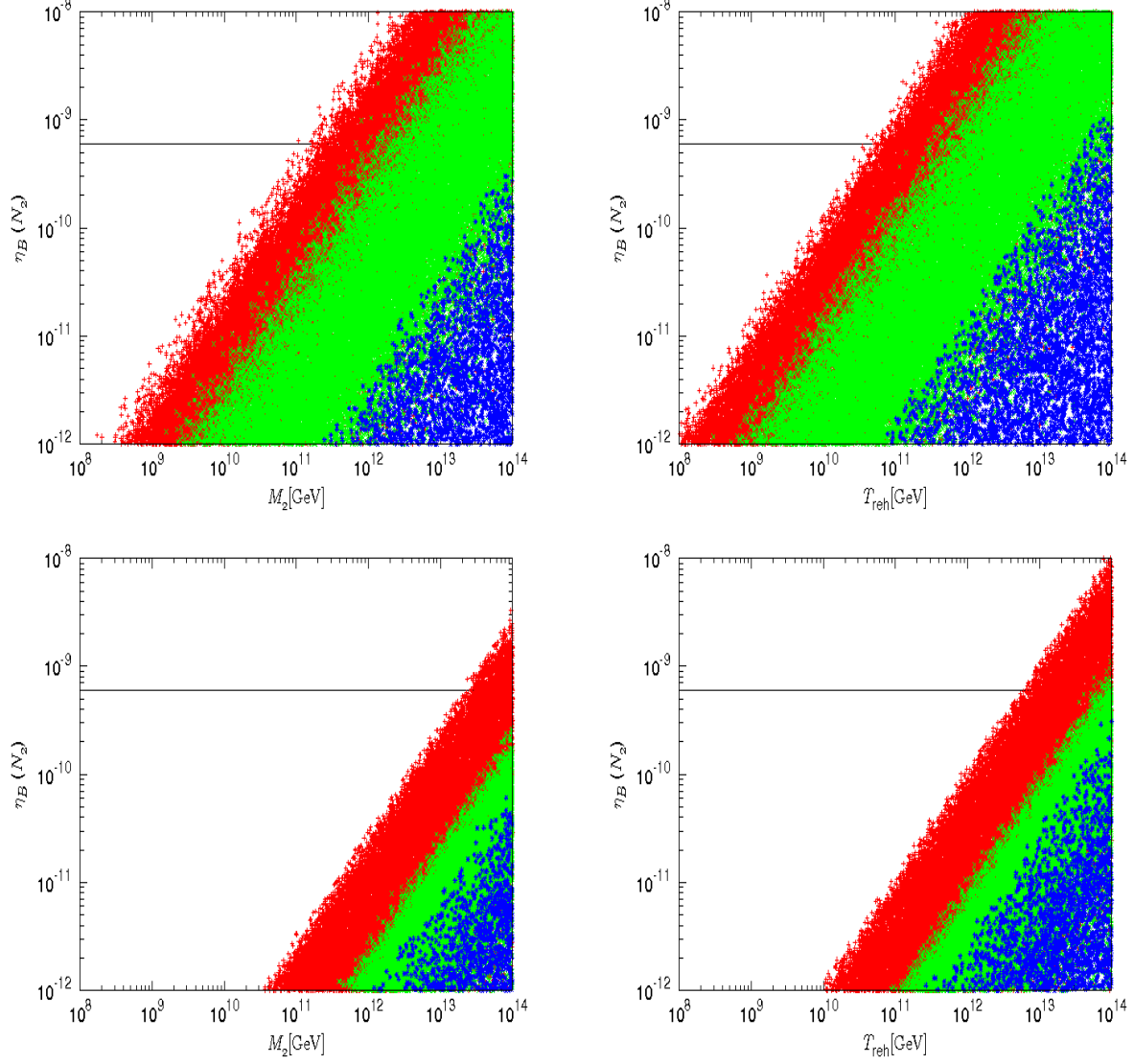


Figure 13: final asymmetry from  $N_2$ -decays versus  $M_2$  (left) and versus the reheat temperature  $T_{\text{reh}}$  (right) for  $|\omega_{32}| = 0$  and  $\omega_{31} \leq 1$ . In the top panels  $\omega_{21} \leq 1$ , while in the bottom panels  $\omega_{21} \leq 0.1$ . The final asymmetry is obtained neglecting the washout term  $w_1(T \sim M_1)$  in the Eq. (63) (red points), calculating it taking into account flavor effects (cf. Eq. (64)) (green points) and neglecting them (blue points).

panels of the same figure and one can see that the lower bound on the reheat temperature is approximately five time more relaxed compared to the lower bound on  $M_2$ .

In the bottom panels we imposed  $|\omega_{21}| \lesssim 0.1$ . One can see that even for such small angles there is still a marginal allowed region. Therefore, only for very small  $|\omega_{21}|$  values one recovers the special case  $\Omega = R_{13}$ .

This result shows that while for  $\Omega = R_{13}$  or for  $\Omega = R_{12}$  the asymmetry from  $N_2$ -decays is always suppressed and the  $N_1$ -dominated scenario holds, as soon as one allows either  $\omega_{31} \neq 0$  or  $\omega_{21} \neq 0$  or both, the asymmetry produced from  $N_2$ -decays can explain the observed asymmetry for acceptable values of  $M_2$ . Even though we did not perform a systematic calculation of the final asymmetry from  $N_2$ -decays in the whole parameter space, in the light of this result it emerges that, if  $10^{11} \text{ GeV} \lesssim M_2 \lesssim 10^{14} \text{ GeV}$ , then the  $N_2$ -dominated scenario seems to be the most natural choice and the validity of the  $N_1$ -dominated scenario relies on unnaturally small complex angles in order to suppress  $\text{Im}[(m_D^\dagger m_D)_{23}]^2$ . We can therefore confirm even in a stronger way what we said in the introduction: it is misleading to talk of a lower bound on  $M_1$  in leptogenesis, while it is more correct to talk of a lower bound on  $T_{\text{reh}}$  holding in the hierarchical limit for  $M_2 \gtrsim 3 M_1$ .

We also notice that this result is not relying crucially on an exact calculation of the washout from  $N_1$ -inverse processes but more on the calculation of the asymmetry produced at  $T \sim M_2$ . In the same Fig. 13 we show (red points) the asymmetry  $\eta_B(N_2)|_{T \sim T_B(K_2)}$ , without the washout, while the green points take into account the washout term  $w_1(T \sim M_1)$  calculated with the Eq. (64). We also show (blue points) the results that would have been obtained calculating the washout neglecting flavor effects.

One can see that the main result relies on the observation that  $\eta_B(N_2)|_{T \sim T_B(K_2)}$  is large already when small  $|\omega_{21}|$  are turned on. A proper calculation of the washout is an important step but somehow a secondary one. Certainly a proper account of flavor effects greatly enhances the asymmetry from  $N_2$ -decays but primarily it is important that there is an asymmetry to be washed out. Notice that an account of the effect envisaged in [48] would produce results somewhere in between the green and the red points. It is certainly important for a precise evaluation but it does not seem to play a crucial role.

Our results show that there is a continuous increase of the asymmetry going from  $\Omega = R_{13}$ , where it vanishes, toward  $\Omega = R_{23}$ . What is important is that as soon as one switches on small  $|\omega_{21}|$  or  $|\omega_{31}|$  the contribution from  $N_2$ -decays is sufficient to explain the observed asymmetry. Going toward the case  $\Omega = R_{23}$  ( $\omega_{21} = \omega_{31} = 0$ ), the allowed region for the  $N_2$ -dominated scenario increases and the lower bound on  $M_2$  relaxes down to a few's  $\times 10^{10} \text{ GeV}$  [5]. We do not see any discontinuity or qualitatively different regime as

envisaged in [22] where the authors distinguish a decoupled regime from a strong washout regime. A proper evaluation of the washout term  $w_1(T \sim M_1)$ , taking into account all kinds of flavor effects [49, 48] is in any case an important ingredient for a correct determination of the border between the domain of validity of the  $N_1$ -dominated scenario and that one of the  $N_2$ -dominated scenario.

## 7 Beyond the hierarchical limit

Finally, in this section we discuss how the bounds change going beyond the hierarchical limit, when  $\delta_2 \equiv (M_2 - M_1)/M_1 \lesssim 2$ . We first neglect flavor effects induced by charged lepton interactions. Notice that there is a second type of flavor effects in the heavy neutrino sector itself [12, 24, 48] due to the fact that for example the lepton quantum state  $|l_2\rangle$  produced by a RH neutrino  $N_2$  does not coincide with  $|l_1\rangle$  produced by a RH neutrino  $N_1$  and in particular  $|l_2\rangle$  does not in general inverse decays with a Higgs to produce a  $N_1$  with the same rate as  $|l_1\rangle$ . We will neglect this effect that would imply that washout terms do not simply add up in the Eq. (16).

Under these assumptions, there are three different effects that change the bounds compared to the hierarchical limit [43]. First of all, in general, one cannot neglect the contribution from the heavier RH neutrinos. Therefore, one cannot just relax the assumption of hierarchical spectrum without also considering the heavier RH neutrino decays. Second, now the addition of washout in the Eq. (16) cannot be neglected. Third, the total  $CP$  asymmetries get typically enhanced compared to their value in the hierarchical limit. The first and third effect tend to increase the final asymmetry relaxing the bounds but the second effect tends to reduce the final asymmetry, making the bounds more stringent. The first two effects saturate for  $\delta_2 \lesssim 0.01$ , the so called degenerate limit, and therefore when  $\delta_2$  decreases below 0.01 only the third effect is left and it changes the bounds in quite a simple way [43], except for some effects studied in [50] in the extreme case of resonant leptogenesis. However, notice that in the case of resonant leptogenesis the bounds simply disappear. Therefore, here we focus especially on the transition between the hierarchical limit and the degenerate limit, for  $0.01 \lesssim \delta_2 \lesssim 2$ . The final asymmetry is given by  $N_{B-L}^f = \sum_i \varepsilon_i \kappa_i^f$ , where  $\varepsilon_1$  is given by the Eq.'s (37)-(40) while, from the Eq. (8), the total  $CP$  asymmetries  $\varepsilon_2$  and  $\varepsilon_3$  are given by

$$\varepsilon_2 = \frac{3}{16\pi} \sum_{j \neq 2} \frac{\text{Im} [(h^\dagger h)_{2j}^2]}{(h^\dagger h)_{22}} \frac{\xi(x_j/x_2)}{\sqrt{x_j/x_2}} \quad \text{and} \quad \varepsilon_3 = \frac{3}{16\pi} \sum_{j \neq 3} \frac{\text{Im} [(h^\dagger h)_{3j}^2]}{(h^\dagger h)_{33}} \frac{\xi(x_j/x_3)}{\sqrt{x_j/x_3}}. \quad (67)$$

The unflavored efficiency factors are given by the Eq. (35) with  $P_{i\alpha}^0 = 1$ ,

$$\kappa_i^f(K_j, \delta_2, \delta_3) = - \int_{z_{\text{in}}}^{\infty} dz' \frac{dN_{N_i}}{dz'} e^{-\int_{z'}^{\infty} dz'' [\Delta W(z'') + \sum_j W_j^{\text{ID}}(z''; K_j)]}, \quad (68)$$

where we defined  $\delta_3 \equiv (M_3 - M_1)/M_1$ . Let us assume that the  $N_i$ -abundances track closely the equilibrium value, so that  $dN_{N_i}/dz \simeq dN_{N_i}^{\text{eq}}/dz$ . This approximation works well for  $K_i \gtrsim 1$ , as we will assume in the following. An approximated expression for  $\kappa_i^f$  is then obtained

$$\kappa_i^f(K_j, \delta_2, \delta_3) \simeq - \int_0^{\infty} dz' \frac{dN_{N_i}^{\text{eq}}}{dz'} \exp \left\{ - \int_{z'}^{\infty} dz'' [\Delta W(z'') + \sum_j W_j^{\text{ID}}(z'')] \right\}. \quad (69)$$

In [5, 43] it was shown that conservatively for

$$\delta_i \gtrsim \delta_{\text{HL}} \equiv \frac{z_B(K_i) + 2}{z_B(K_1) - 2} - 1, \quad (70)$$

one can assume the hierarchical limit for the calculation of  $\kappa_i^f$ . In this case the washout from the RH neutrinos  $l \neq i$  lighter than  $N_i$  is factorized and (cf. Eq. (44))

$$\kappa_i^f \simeq \kappa(K_i) e^{-\int_0^{\infty} dz' \sum_l W_l^{\text{ID}}(z')}. \quad (71)$$

On the other hand the washout from the  $N_i$ -inverse processes on the asymmetry produced by  $N_l$ -decays is negligible and

$$\kappa_{l_*}^f \simeq - \int_{z_{\text{in}}}^{\infty} dz' \frac{dN_{N_{l_*}}}{dz'} e^{-\int_{z'}^{\infty} dz'' [\Delta W(z'') + \sum_l W_l^{\text{ID}}(z''; K_l)]}, \quad (72)$$

where with  $N_{l_*}$  we indicated one particular  $N_l$ . Typically one has  $\delta_{\text{HL}} \simeq 2$  and this is the reason why we always used  $M_2 \gtrsim 3 M_1$  as a condition for the hierarchical limit to hold. On the contrary, if  $(M_i - M_l)/M_i \lesssim 0.01$ , then one recovers the degenerate limit where  $\kappa_i^f \simeq \kappa_l^f(K_i + K_l, K_{j \neq i, l})$ . There are three different cases: a partial degenerate limit with  $\delta_2 \lesssim 0.01$ , a partial degenerate limit with  $(M_3 - M_2)/M_2 \lesssim 0.01$  and a full degenerate limit where  $\delta_3 \lesssim 0.01$ . In this last case one has simply

$$\kappa_1^f = \kappa_2^f = \kappa_3^f \simeq \kappa(K_1 + K_2 + K_3). \quad (73)$$

We will now focus on two particular choices for  $M_3$  but without imposing any restriction on  $\delta_2$ . The *first case* we consider is  $M_3 \gg M_2 \simeq M_1$ . This was also studied in [43] but for two particular choices of the orthogonal matrix, while here we do not make any assumption on  $\Omega$ . The contribution from the heaviest RH neutrino is negligible both

because  $\kappa_3^f \ll \kappa_1^f, \kappa_2^f$  and because  $\varepsilon_3 \ll \varepsilon_1, \varepsilon_2$ . The washout of  $N_3$ -inverse processes on the asymmetry produced from the two lightest RH neutrino decays is negligible as well.

Two convenient fits for  $\kappa_1^f$  and  $\kappa_2^f$  can be used [43],

$$\kappa_1^{\text{fit}}(K_1, K_2, \delta_2) = \frac{2}{z_B(K_1 + K_2^{(1-\delta_2)^3})(K_1 + K_2^{1-\delta_2})} \quad (74)$$

and

$$\kappa_2^{\text{fit}}(K_1, K_2, \delta_2) = \frac{2 \left[ \frac{1-\delta_2}{(1-\delta_2)^2} \right]}{z_B(K_2 + K_1^{(1-\delta_2)^3})(K_2 + K_1^{1-\delta_2})} \times e^{-\frac{3\pi}{8} K_1 \left( \frac{\delta_2}{1+\delta_2} \right)^{2.1}}. \quad (75)$$

For  $M_3 \gg M_2$  the Eq. (67) for  $\varepsilon_2$  can be further specialized into

$$\varepsilon_2 \simeq \bar{\varepsilon}(M_2) \frac{\text{Im} [\sum_h m_h \Omega_{h2}^* \Omega_{h3}]^2}{\tilde{m}_2 m_{\text{atm}}} + \bar{\varepsilon}(M_1) \frac{\text{Im} [\sum_h m_h \Omega_{h2}^* \Omega_{h1}]^2}{\tilde{m}_2 m_{\text{atm}}} \xi \left( \frac{1}{x_2} \right). \quad (76)$$

If  $\delta_2 \ll 1$  and if one maximizes over the  $\Omega$  parameters, the first term can be neglected and since  $\xi(1/x_2) \simeq -\xi(x_2)$ , the expression simplifies into

$$\max_{\Omega}[\varepsilon_2] \simeq -\bar{\varepsilon}(M_1) \xi(x_2) \beta_2(m_1), \quad \beta_2(m_1) \equiv \max_{\Omega} \left[ \frac{\text{Im} [\sum_h m_h \Omega_{h2}^* \Omega_{h1}]^2}{\tilde{m}_2 m_{\text{atm}}} \right]. \quad (77)$$

While  $\varepsilon_1$  gets suppressed when  $m_1$  increases (cf. Eq. (49)), the function  $\beta_2(m_1)$  in general does not and therefore, at large  $m_1$ , it gives the dominant contribution to the maximum asymmetry determining the bounds in the plane  $(m_1, M_1)$  that are shown in Fig. 14 for  $\delta_2 = 1, 0.1, 0.05, 0.01$  and where we imposed a strong washout condition. This automatically guarantees the validity of the fits (74) and (75) for the efficiency factors. The results in the unflavored case correspond to the green points. One can notice a result already found in [43] that we confirm here in a more general way. For  $\delta_2 \sim 0.1$  the washout addition makes the lower bound on  $M_1$  even slightly more stringent while only for  $\delta_2 \lesssim 0.01$  the lower bound gets clearly more relaxed. On the other hand, concerning the upper bound on  $m_1$ , the fact that  $\varepsilon_2$  increases with  $m_1$  implies that the upper bound on  $m_1$  gets relaxed already at  $\delta_2 \simeq 0.1$ .

Let us now turn to study the *second case* when  $M_3 = M_2$ . This time the heaviest RH neutrinos contribute both to the asymmetry production and to the washout. Having the expressions for the case  $M_3 \gg M_2$ , it is easy to derive the efficiency factors in the partial degenerate limit  $(M_3 - M_2)/M_2 \lesssim 0.01$ . Indeed if  $i = 2, 3$ , one has simply

$$\begin{aligned} \kappa_3^f \simeq \kappa_2^f &\simeq - \int_0^\infty dz' \frac{dN_{N_i}^{\text{eq}}}{dz'} \times \\ &\times \exp \left\{ - \int_{z'}^\infty dz'' [\Delta W(z'') + W_1^{\text{ID}}(z''; K_1) + W_i^{\text{ID}}(z''; K_2 + K_3)] \right\} \\ &\simeq \kappa_2^{\text{fit}}(K_1, K_2 + K_3, \delta_2). \end{aligned} \quad (78)$$

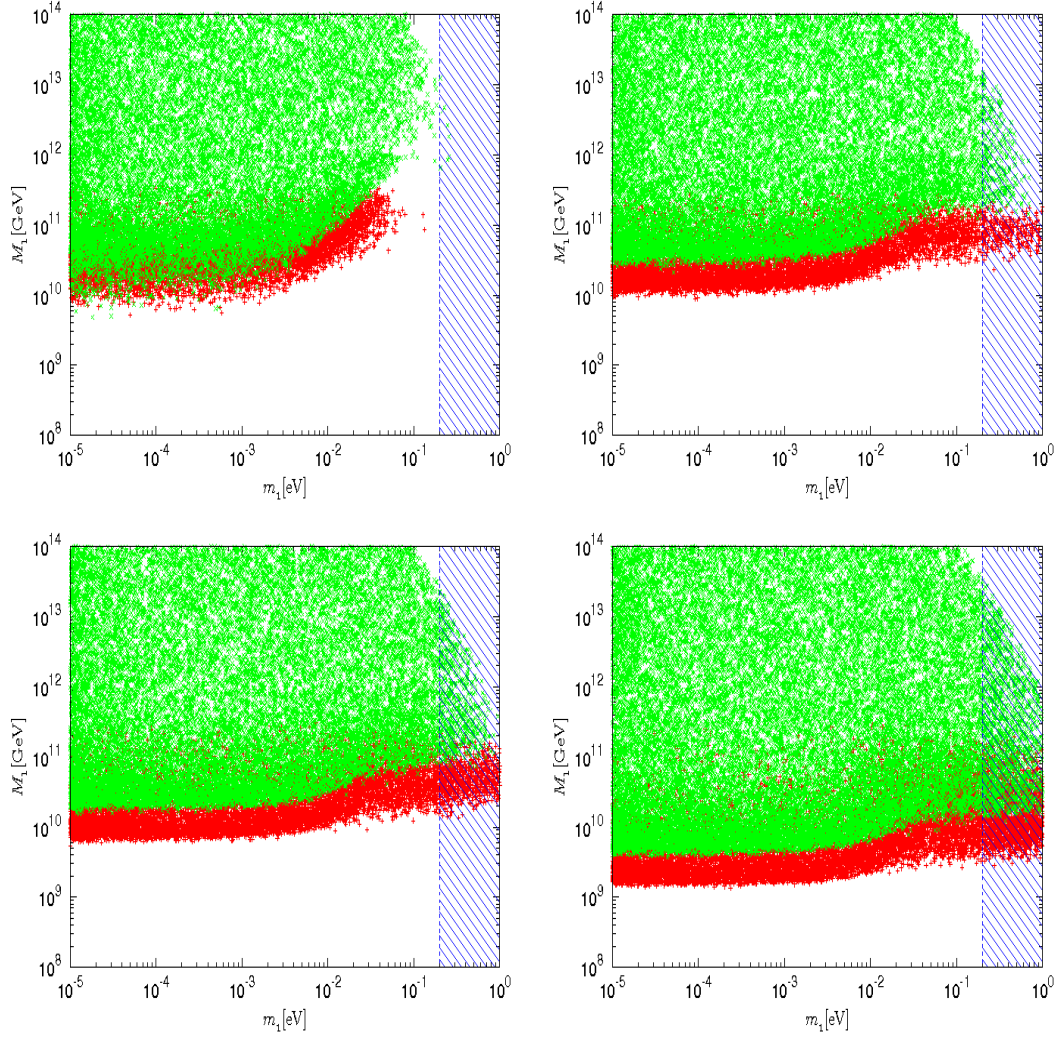


Figure 14: Allowed region in the  $(m_1, M_1)$  plane for the case  $M_3 \gg M_2$  in the unflavored case (green points) and in the fully flavored regime imposing the condition Eq. (36) (red points) for  $\delta_2 = 1$  (top-left), 0.1 (top-right), 0.05 (bottom-left) and 0.01 (bottom-right).

The calculation of the total  $CP$  asymmetries  $\varepsilon_2$  and  $\varepsilon_3$  is slightly more involved. If we assume that  $M_2 = M_3$  exactly, then the interference term between  $N_2$  and  $N_3$  vanish, though notice that the expression Eq. (8) for  $\varepsilon_2$  and  $\varepsilon_3$  diverge for  $M_2 = M_3$  because they hold only for mass differences less than the decay widths. Therefore, one has

$$\varepsilon_{i=2,3} \simeq \xi(x_2) \bar{\varepsilon}(M_1) \left[ \frac{\sum_h m_h^2 \text{Im}[\Omega_{hi}^* \Omega_{h1}^2]}{\tilde{m}_i m_{\text{atm}}} + 2 \sum_{h<l} m_h m_l \frac{\text{Im}[\Omega_{h1} \Omega_{l1} \Omega_{hi}^* \Omega_{li}^*]}{\tilde{m}_i m_{\text{atm}}} \right]. \quad (79)$$

In passing let us notice that, without the interference term between  $N_2$  and  $N_3$ , the asymmetries vanish for  $M_1 \rightarrow 0$ . The final asymmetry can then be written as

$$\begin{aligned} N_{B-L}^f &= \xi(x_2) \bar{\varepsilon}(M_1) \left\{ \kappa_1^{\text{fit}}(K_1, K_2; \delta_2) \beta(m_1, \Omega) + \kappa_2^{\text{fit}}(K_1, K_2 + K_3, \delta_2) \times \right. \\ &\quad \times \left[ \frac{\sum_h m_h^2 \text{Im}[\Omega_{h2}^* \Omega_{h1}^2]}{\tilde{m}_2 m_{\text{atm}}} + \frac{\sum_h m_h^2 \text{Im}[\Omega_{h3}^* \Omega_{h1}^2]}{\tilde{m}_3 m_{\text{atm}}} \right] \\ &\quad \left. + 2 \sum_{h<l} m_h m_l \frac{\text{Im}[\Omega_{h1} \Omega_{l1} \Omega_{h3}^* \Omega_{l3}^*]}{m_{\text{atm}}} \left( \frac{\tilde{m}_2 - \tilde{m}_3}{\tilde{m}_2 \tilde{m}_3} \right) \right\}. \quad (81) \end{aligned}$$

Notice that if  $\tilde{m}_2 = \tilde{m}_3$ , then  $\varepsilon_2 + \varepsilon_3 = (\tilde{m}_2/\tilde{m}_1) \varepsilon_1 \propto (m_3 - m_1)$  and therefore the contribution from the two heavier RH neutrinos is suppressed as well. This makes the bounds more stringent compared to the case  $M_3 \gg M_2$ , especially for  $\delta_2 \sim 0.1$ . In Fig. 15 we show the bounds in the case  $M_2 = M_3$  again for  $\delta_2 = 1, 0.1, 0.05, 0.01$ . One can see that now for  $\delta_2 \sim 0.1$  not only the lower bound on  $M_1$  does not get relaxed but also the upper bound on  $m_1$  (green points). Again, for  $\delta_2 \lesssim 0.01$ , both the  $M_1$  lower bound and the  $m_1$  upper bound get clearly relaxed.

Both in the case  $M_3 \gg M_2$  and in the case  $M_3 = M_2$ , we repeated the calculations also in the fully flavored regime. Now the final asymmetry has to be calculated using

$$N_{B-L}^f = \sum_{\alpha,i} \varepsilon_{i\alpha} \kappa_{i\alpha}^f \simeq \sum_i N_{\text{fl}}^i \bar{\varepsilon}_i \kappa_i^f + \frac{1}{2} \sum_i \Delta P_{i\alpha} [\kappa_{i\alpha}^f - \kappa_{i\beta}^f], \quad (82)$$

where we generalized the approximated form we already used in the hierarchical limit (cf. Eq. (50)).

In the case  $M_3 \gg M_2$ , the contribution from  $N_3$ -decays is this time less trivially negligible because in principle the washout from the the two lighter RH neutrinos could be weaker in one flavor and because moreover the flavored  $CP$  asymmetries  $\varepsilon_{3\alpha}$ , contrarily to the total  $\varepsilon_3$ , are not necessarily suppressed in the hierarchical limit [6]. However, it turns out that the contribution from  $N_3$ -decays is too small to explain the observed asymmetry and it can be therefore neglected in the determination of the bounds.

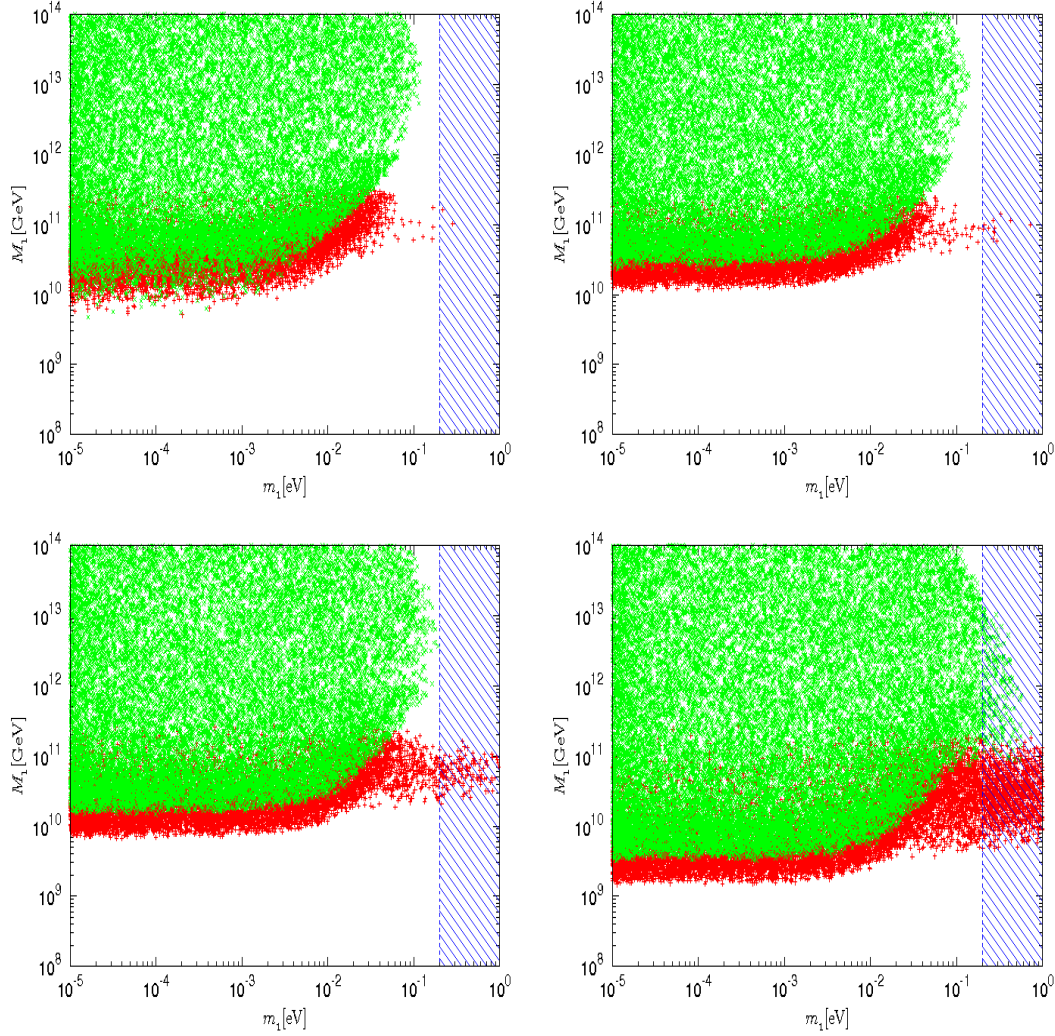


Figure 15: Allowed region in the  $(m_1, M_1)$  plane for  $M_2 = M_3$  in the unflavored case (green points) and in the fully flavored regime imposing the condition Eq. (36) (red points) for  $\delta_2 = 1$  (top-left), 0.1 (top-right), 0.05 (bottom-left) and 0.01 (bottom-right). We are also imposing  $|\omega_{ij}| \leq 1$  and  $K_{\alpha i} \gtrsim 1$ .



Assuming  $K_{\alpha i} \gtrsim 1$ , expressions for the flavored efficiency factors can be obtained from the unflavored ones just replacing  $K_i \rightarrow K_{i\alpha} \equiv P_{i\alpha}^0 K_i$ . In this way we can use the approximation (69) and the fits Eq. (74) and (75) with  $K_i$  replaced by  $K_{i\alpha}$ .

In Fig. 14 one can see how flavor effects affect the bounds (red points). For  $\delta_2 = 1$  there is no relaxation of the lower bound on  $M_1$ , since the hierarchical limit still holds and because at the onset of the strong washout there is no relaxation due to flavor effects for  $|\omega_{ij}| < 1$  [6], as we are imposing. For  $\delta_2 \ll 1$  and  $m_1 \lesssim 0.01$  eV one can see that there is a factor two relaxation. The reason is that the asymmetry is not maximized in a one flavor dominance case but in a democratic case, that means for values of the parameters where the only change to the final asymmetry from flavor effects is described by the enhancement of a factor  $N_{\text{fl}}^i \simeq 2$ , while the additional terms  $\propto \Delta P_{i\alpha} (\kappa_{i\alpha} - \kappa_{i\beta})$  vanish. On the other hand, for  $m_1 \gtrsim 0.01$  eV, one flavor dominance makes possible a large enhancement of the asymmetry and this is why the upper bound on  $m_1$  is much more relaxed. Similar results hold in the case  $M_2 = M_3$ , as one can see from Fig. 15.

## 8 Conclusions

The simple vanilla leptogenesis scenario grasps important features of leptogenesis bounds but misses many important effects. Assuming the  $N_1$ -dominated scenario, the lower bound on  $M_1$  seems to be a solid feature and we have seen that it resists even for heavy neutrino mass degeneracies as small as  $\delta_2 \sim 0.01$ . However, our analysis revealed that flavor effects introduce new  $CP$  violating terms that relax the bound of one order of magnitude for acceptable choices of the parameters and still within the hierarchical limit. Flavor effects modify the upper bound on  $m_1$  as well but, as we stressed, an ultimate answer requires solutions of more general kinetic equations that should be able to describe the intermediate regime where the coherence of the final quantum lepton state is lost but a full decoherence is still not achieved. We have seen that an account of the Higgs asymmetry supports such a prudent conclusion.

Still within the hierarchical limit but accounting for the asymmetry produced from the  $N_2$ -decays, the lower bound on  $M_1$  disappears and is replaced by a lower bound on  $M_2$  that still implies a lower bound on the reheat temperature. We showed some more general conditions for the validity of the  $N_1$ -dominated scenario and of the lower bound on  $M_1$ . For example the  $N_1$ -dominated scenario certainly applies in the popular two effective RH neutrino limit, for  $M_3 \gg 10^{14}$  GeV, that implies that the heaviest RH neutrino decouples. However, apart from this case, our analysis indicates that a  $N_2$ -dominated scenario is a more natural option and that neglecting the asymmetry from  $N_2$ -decays can be a wrong

assumption.

In conclusion, our analysis answered many different questions about the bounds on neutrino masses that are obtained within the leptogenesis scenario based on the simplest version of the see-saw mechanism. Despite many proposed extensions, this still represent the most attractive possibility since it realizes a successful link between the neutrino masses and the observed asymmetry where the measured values exhibit an interesting conspiracy. The discovery of  $CP$  violating effects in neutrino oscillations or in lepton decays, the determination of the absolute neutrino mass scale and of the neutrino mass spectrum ordering, normal or inverted, will likely provide further interesting tests during next years, making current experimental ‘coincidences’ even stronger or forcing departures from the minimal picture.

### Acknowledgments

We wish to thank A. Riotto for many useful discussions. PDB is supported by the Helmholtz Association of National Research Centres, under project VH-NG-006.

## References

- [1] M. Fukugita, T. Yanagida, Phys. Lett. **B 174** (1986) 45.
- [2] P. Minkowski, Phys. Lett. B **67** (1977) 421; T. Yanagida, in *Workshop on Unified Theories*, KEK report 79-18 (1979) p. 95; M. Gell-Mann, P. Ramond, R. Slansky, in *Supergravity* (North Holland, Amsterdam, 1979) eds. P. van Nieuwenhuizen, D. Freedman, p. 315; S.L. Glashow, in *1979 Cargese Summer Institute on Quarks and Leptons* (Plenum Press, New York, 1980) p. 687; R. Barbieri, D. V. Nanopoulos, G. Morchio and F. Strocchi, Phys. Lett. B **90** (1980) 91; R. N. Mohapatra and G. Senjanovic, Phys. Rev. Lett. **44** (1980) 912.
- [3] S. Davidson and A. Ibarra, Phys. Lett. B **535** (2002) 25.
- [4] W. Buchmüller, P. Di Bari and M. Plümacher, Nucl. Phys. B **643** (2002) 367.
- [5] P. Di Bari, Nucl. Phys. B **727** (2005) 318.
- [6] S. Blanchet and P. Di Bari, JCAP **03** (2007) 018.
- [7] W. Buchmüller, P. Di Bari and M. Plümacher, Annals Phys. **315** (2005) 305.
- [8] G. F. Giudice, A. Notari, M. Raidal, A. Riotto and A. Strumia, Nucl. Phys. B **685** (2004) 89.

- [9] W. Buchmuller, P. Di Bari and M. Plumacher, Nucl. Phys. B **665** (2003) 445.
- [10] E. Nardi, Y. Nir, E. Roulet and J. Racker, JHEP **0601** (2006) 164.
- [11] A. Abada, S. Davidson, F. X. Josse-Michaux, M. Losada and A. Riotto, JCAP **0604** (2006) 004
- [12] R. Barbieri, P. Creminelli, A. Strumia and N. Tetradis, Nucl. Phys. B **575** (2000) 61.
- [13] T. Endoh, T. Morozumi and Z. h. Xiong, Prog. Theor. Phys. **111** (2004) 123; A. Pilaftsis and T. E. J. Underwood, Phys. Rev. D **72** (2005) 113001 O. Vives, Phys. Rev. D **73** (2006) 073006.
- [14] A. Abada, S. Davidson, A. Ibarra, F. X. Josse-Michaux, M. Losada and A. Riotto, JHEP **0609** (2006) 010.
- [15] S. Pascoli, S. T. Petcov and A. Riotto, Phys. Rev. D **75** (2007) 083511.
- [16] S. Pascoli, S. T. Petcov and A. Riotto, Nucl. Phys. B **774** (2007) 1.
- [17] G. C. Branco, R. Gonzalez Felipe and F. R. Joaquim, Phys. Lett. B **645** (2007) 432.
- [18] S. Antusch and A. M. Teixeira, JCAP **0702** (2007) 024.
- [19] A. Anisimov, S. Blanchet and P. Di Bari, JCAP **0804** (2008) 033.
- [20] S. Blanchet, P. Di Bari and G. G. Raffelt, JCAP **03** (2007) 012.
- [21] A. De Simone and A. Riotto, JCAP **0702** (2007) 005.
- [22] S. Davidson, E. Nardi and Y. Nir, arXiv:0802.2962 [hep-ph].
- [23] K. Hamaguchi, H. Murayama and T. Yanagida, Phys. Rev. D **65** (2002) 043512.
- [24] T. Hambye, Y. Lin, A. Notari, M. Papucci and A. Strumia, Nucl. Phys. B **695** (2004) 169
- [25] S. Davidson and R. Kitano, JHEP **0403** (2004) 020.
- [26] M. C. Gonzalez-Garcia and M. Maltoni, Phys. Rept. **460** (2008) 1.
- [27] E. Komatsu *et al.* [WMAP Collaboration], arXiv:0803.0547 [astro-ph].

- [28] A. D. Sakharov, Pisma Zh. Eksp. Teor. Fiz. **5** (1967) 32
- [29] V. A. Kuzmin, V. A. Rubakov, M. E. Shaposhnikov, Phys. Lett. **B 155** (1985) 36.
- [30] L. Covi, E. Roulet, F. Vissani, Phys. Lett. **B 384** (1996) 169.
- [31] B. A. Campbell, S. Davidson, J. R. Ellis and K. A. Olive, Phys. Lett. B **297** (1992) 118; J. M. Cline, K. Kainulainen and K. A. Olive, Phys. Rev. D **49** (1994) 6394.
- [32] A. D. Dolgov and Ya. B. Zeldovich, Rev. Mod. Phys. **53** (1981) 1; E. W. Kolb and S. Wolfram, Nucl. Phys. B **172** (1980) 224, *ibid.* **B 195** (1982) 542 (E).
- [33] M. A. Luty, Phys. Rev. D **45** (1992) 455.
- [34] W. Buchmüller and M. Plümacher, Phys. Lett. B **511** (2001) 74
- [35] E. Nardi, Y. Nir, J. Racker and E. Roulet, JHEP **0601** (2006) 068
- [36] J. A. Casas and A. Ibarra, Nucl. Phys. B **618** (2001) 171.
- [37] S. Eidelman et al., Phys. Lett. **B592**, 1 (2004) (URL:<http://pdg.lbl.gov/>).
- [38] M. Fujii, K. Hamaguchi and T. Yanagida, Phys. Rev. D **65** (2002) 115012.
- [39] F. del Aguila, J. A. Aguilar-Saavedra, A. Martinez de la Ossa and D. Meloni, Phys. Lett. B **613** (2005) 170; J. Kersten and A. Y. Smirnov, Phys. Rev. D **76** (2007) 073005.
- [40] P. H. Frampton, S. L. Glashow and T. Yanagida, Phys. Lett. B **548** (2002) 119; M. Raidal and A. Strumia, Phys. Lett. B **553** (2003) 72; A. Ibarra and G. G. Ross, Phys. Lett. B **575** (2003) 279.
- [41] P. H. Chankowski and K. Turzyski, Phys. Lett. B **570** (2003) 198.
- [42] P. H. Chankowski, J. R. Ellis, S. Pokorski, M. Raidal and K. Turzyski, Nucl. Phys. B **690** (2004) 279; S. T. Petcov, W. Rodejohann, T. Shindou and Y. Takanishi, Nucl. Phys. B **739** (2006) 208.
- [43] S. Blanchet and P. Di Bari, JCAP **0606** (2006) 023.
- [44] P. Di Bari, AIP Conf. Proc. **655** (2003) 208 [arXiv:hep-ph/0211175]. P. Di Bari, [arXiv:hep-ph/0406115].
- [45] W. Buchmüller, P. Di Bari and M. Plumacher, New J. Phys. **6** (2004) 105.

- [46] E. Molinaro and S. T. Petcov, arXiv:0803.4120 [hep-ph].
- [47] E. Molinaro, S. T. Petcov, T. Shindou and Y. Takahashi, Nucl. Phys. B **797** (2008) 93.
- [48] G. Engelhard, Y. Grossman, E. Nardi and Y. Nir, Phys. Rev. Lett. **99** (2007) 081802.
- [49] O. Vives, Phys. Rev. D **73** (2006) 073006.
- [50] A. De Simone and A. Riotto, JCAP **0708** (2007) 013.